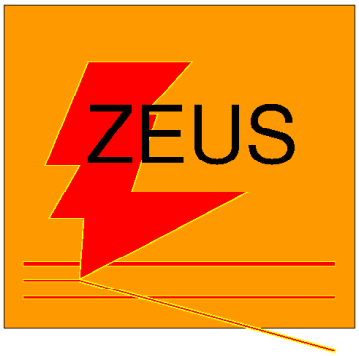

ZEUS PROGRESS REPORT

MAY 2000 − JULY 2002

ZEUS UK COLLABORATION

17th June 2002

1 Introduction

The upgrade to the HERA accelerator that will provide a five-fold increase in luminosity and lepton-beam polarisation for the colliding beam experiments was carried out in 2000 and 2001. Commissioning of the upgraded electron and proton rings began in August 2001 and first collisions were observed in the ZEUS interaction region in October 2001.

The ZEUS detector upgrade was also completed during the long shutdown in 2000-01. The silicon microvertex detector (MVD), in which the UK has a significant role, was completed, installed and commissioned and the forward tracking system was augmented with a straw tube tracker. The upgrade of the transverse polarimeter (TPOL), where the UK has a leading role, was also completed. Currently HERA is concentrating on commissioning luminosity with acceptable backgrounds to the experiments. Although this has taken longer than hoped, steady progress is being made.

The UK groups continue to have responsibility for the operation and maintenance of the Central Tracking Detector (CTD) that was built in the UK and is equipped with trigger and readout electronics designed and manufactured in the UK. It is essential that we continue to have the resources to maintain the performance of the CTD at its present high standard since the tracking information it provides is vitally important for ZEUS triggering and for all physics analyses. ZEUS data taking is inhibited unless the CTD is active.

Members of the UK groups are contributing strongly to the background monitoring that is vital to allow the remaining obstacles to luminosity running to be removed. We expect to begin routine luminosity operation in the near future. As a result, the emphasis of the UK groups has shifted from re-commissioning the CTD and commissioning the new MVD and TPOL hardware to the preparation of the analysis programmes needed for high-statistics, high-precision HERA II data.

The UK groups continue to make a strong contribution to both the preparations for data-taking and to data-taking itself. The UK provided the two person 'pre-run' coordinator team which has been vital in re-establishing data-taking in the experiment. We provide a good proportion of the shift leaders (4 units) and deputy shift leaders (2 units). The UK continues to take responsibility for a wide range of activities within the ZEUS collaboration: the ZEUS spokesman is a UK physicist; the UK provided the ZEUS tracking coordinator, the Monte Carlo code manager, the Monte Carlo coordinator, the CTD coordinator and the straw tube tracker on-line expert; UK physicists are joint coordinators for three of the five ZEUS physics groups.

This report is structured as follows: the CTD status and infrastructure are covered in section 2; the UK contributions to the MVD and the TPOL are covered in sections 3 and 4; physics results with UK involvement in section 5 and future plans and resources requested in section 6. Lists of publications, theses, the membership of ZEUS-UK groups, our computing request and the ZEUS organogram are contained in the appendices.

2 Central tracking detector status and infrastructure

The Central Tracking Detector (CTD) is a large−volume, cylindrical drift chamber covering the central region $15^o < \theta < 164^o$. It provides charged−particle tracking, momentum measurement and particle identification through dE/dx. It also participates in all three levels of the ZEUS trigger.

The CTD's 4608 sense wires are arranged in nine superlayers, superlayer one being the innermost. The wires in odd-numbered superlayers run parallel to the chamber axis, whilst those in even-numbered layers have a small stereo angle ($\sim \pm 5^o$). Taken together they provide sufficient information to reconstruct tracks in three dimensions. All sense wires in the chamber are equipped with Flash Analogue-to-Digital Conversion (FADC) electronics and, in

addition, all wires in superlayer one and the odd-numbered wires in superlayers three and five have z-by-timing electronics for the first-level trigger.

During the shutdown for the HERA upgrade the CTD was flushed with argon:CO_2. Despite not being operated for ten months, it was successfully re-commissioned in cosmic ray tests of the ZEUS microvertex detector in July 2001 and has subsequently performed very reliably even in the very poor background conditions characteristic of the initial data-taking period.

The continued operation and reliability of the CTD is of utmost importance to ZEUS. The chamber has been ready for data-taking in the new HERA environment since the end of 2001 and has already been providing vital information for the commissioning of the upgraded HERA machine. The CTD will remain at the heart of ZEUS and the ZEUS physics program for the remaining lifetime of the experiment.

2.1 Triggering

ZEUS operates a three−level trigger. UK physicists are intimately involved in the ZEUS trigger, particularly at the first and second levels. The first level trigger is a hardware−based system the principal aim of which is to reduce backgrounds that do not arise from *ep* collisions. CTD information is essential for this and the detector uses dedicated, pipelined processor cards that provide tracking information to the global first−level trigger. The CTD first−level trigger operated reliably during running in 2000 and has been successfully recommissioned following the long shutdown.

The ZEUS second-level trigger uses more precise software algorithms to clean the event sample further and classify certain types of physics events. Detailed tracking information is provided by the CTD second-level trigger which makes use of the data from all five axial superlayers and the z-by-timing information from layers 1, 3 and 5. A precise measurement of the event vertex at the second level is a powerful technique for rejection of background. Before the long shutdown, modifications were made to the CTD transputer network to allow data from the FADC electronics to be sent to the Global Tracking Trigger (GTT, see section 3). This system will combine CTD data with the precise information from the new microvertex detector to provide a very accurate event vertex measurement. The CTD SLT has been successfully recommissioned and the link to the GTT computer systems has now been successfully tested.

The third-level trigger (TLT) runs on a farm of Unix workstations and PCs using an appropriate version of the off-line reconstruction code. The CTD TLT code is an optimised version of the full off-line reconstruction. Its performance is only slightly below that of the off-line version and aids monitoring of the system by providing early warning of any changes in critical CTD parameters.

As part of a successful small collaboration with Argonne National Laboratory (through a DoE funded UK studentship) we have also contributed to the re-commissioning of the calorimeter first level trigger processor (CFLTP). The CFLTP is the heart of the calorimeter first level trigger, processing 3 Gbytes of data per second and allowing ZEUS to trigger on energy sums with great speed and flexibility. The CFLTP is essential to data taking.

2.2 Infrastructure and monitoring

In general the CTD support infrastructure has performed very well. The CTD water cooling circuit is now fully operational again. A blocked pipe to the forward end plate was cleared by "sucking" the blockage out of the system. The water flow rates through both arms of the cooling system are

now well above the minimum required to cool the CTD and show no signs of further fall off. Fine filters are also now installed between the main ZEUS cooling circuit and the input to the CTD water cooling system which will prevent further problems.

The gas system operated reliably throughout the long shutdown. After the cosmic tests some fluctuations in the gas composition were observed. The problem was traced to a faulty mass flow controller, which has now been replaced. The flow meters on the gas system have also been replaced as part of its ongoing maintenance.

New uninterruptible power supplies (UPS) have also been installed in the CTD high-voltage (HV) system. These new UPSs will provide increased protection from power failures and are more reliable than the previous units.

Since water was added to the gas mixture to overcome the Malter effect (as detailed in our last submission to the PPESP) the chamber has shown no further sign of HV instability. The addition of water caused some shift in the operating parameters of the CTD, including the reduction of the Lorentz angle to 41^{o} from the nominal value of 45^{o}. After some investigation, it proved possible to restore the Lorentz angle by modifying the gas composition (reducing the CO_2 composition by 2% and increasing the ethane by 2% whilst keeping the argon fraction constant) and increasing the drift field. The chamber is now operating efficiently once more and will continue to run with water in the gas mixture for the lifetime of ZEUS.

Over the course of the shutdown the ZEUS data-acquisition environment has been upgraded to operate with the larger data-rates expected in the post-upgrade environment. In particular, the ZEUS event builder (EVB), a system that assembles the complete data for an event from all the sub-components of the detector, has been replaced with a new system. The CTD was the first pre-upgrade component to move to the new EVB and is operating successfully with it.

ZEUS has implemented a system for automatic online data monitoring. For the CTD, this is done by checking a small number of critical histograms which are also made available to the shift crew. The automatic histogram checking was initially incorporated into the CTD online program, but will be moved to a dedicated machine in future for ease of maintenance and development. More detailed monitoring is performed off-line using samples of the data which are automatically analysed and then checked by a small team of experts. This system has proved to be effective over a number of years in the early diagnosis of problems. It also provides calibration constants for the CTD and quality control of the CTD data used for physics analysis.

3 ZEUS microvertex detector

ZEUS UK groups have been involved in the ZEUS Microvertex Detector (MVD) project with responsibility, on the hardware side, for: the MVD installation; the clock and control electronics; the laser alignment system and a cable 'patchbox'. On the software side we wrote the local run control, event display and histogramming packages, and are involved in the development of a second−level global track trigger (GTT). We are also involved in offline precision alignment using track data.

A summary of the status of the MVD project as a whole is given by Fig. 1, which shows an event from a luminosity run in May 2002 with tracks and hits in both the CTD and the MVD.

3.1 Clock and control

The ZEUS−UK group provided the clock and control system for the MVD. This system consists of three main subsystems: a master controller and slave in each of the ADC crates; sixteen driver

boards in a crate of their own; twenty−four distribution cards in the patch boxes close to the detector. In addition, we provided the power supplies associated with each of these systems.

The master and slave system consists principally of digital logic on programmable devices. It: (a) receives clock and trigger signals from the ZEUS global first level trigger (GFLT); (b) sends clock, trigger and reset signals to the HELIX driver system; (c) receives busy and error signals from the ADCs and sends them to the GFLT. We provided a ZEUS trigger simulator, in the same crate as the master board, which allows standalone running. The master board also allows an external trigger to be input to the front panel. This facility was used during cosmic ray data taking on the test stand.

The HELIX driver system (16 6U VME cards) fans out signals from the master and sends them as Low Voltage Differential Signals (LVDS) down approximately 20m of cable to the patch box cards. The system also interfaces with the MVD slow control system to allow calibration data to be sent to the detector chips at the start of a run and provides monitoring information.

The patchbox cards comprise three cards for the control signals and three for the clock signals in each of the four patch boxes. These cards amplify the signals from the HELIX drivers and convert the control signals to single ended CMOS as required by the HELIX chips. These cards form part of the challenging patchbox system (see below) and were designed and installed by us.

The whole system was delivered on schedule, in time for cosmic ray testing in January 2001 in the test area and is now fully installed and functional in the ZEUS hall.

3.2 The patchbox

The patchbox was not in the original proposal to the PPESP, but was a key component on the critical path of the MVD project. Owing to space limitations from existing components in ZEUS and the new magnets for the final focus, the nearest location for the main readout electronics was nearly 30 m from the detector. Clearly, a cable connection station (the ’patchbox’) was needed. The specifications for the patchbox were that it should:

1. fit inside the very limited space available around the rear beam pine;
2. rearrange the cables from wafer−grouped on the MVD side to function−grouped (readout, clock−and−control, bias voltage, etc.) on the readout side;
3. rigorously screen all MVD cables (high voltage, low voltage, clock−and−control, analogue readout) to avoid pickup in the hostile electronic environment near the beam line;
4. boost the clock−and−control signals (see previous section).

A very ingenious design of four doubly-insulated crates with a specially designed back-plane was devised. The boxes were ready for the MVD ‘full system test’ at DESY (December 2000 — March 2001) and then had to be uncabled, moved to the ZEUS hall, installed and recabled. Full testing of all MVD cables was required at each stage.

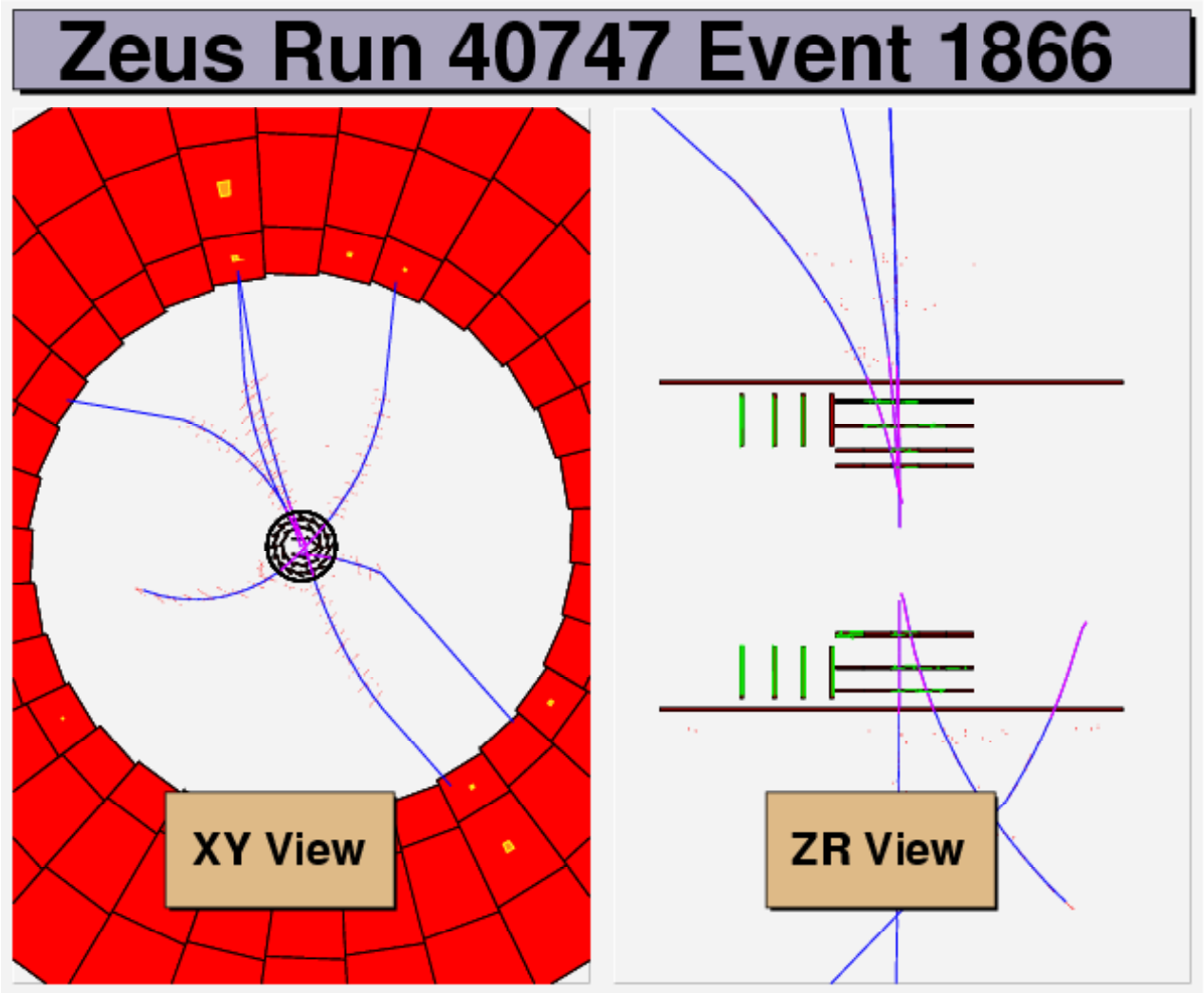

Figure 1: An event from a luminosity run in May 2002, showing tracks fitted to hits in both the CTD and MVD barrel region.

3.3 Alignment

The installation of the MVD was another UK responsibility. We provided the laser alignment system [1] for the new microvertex detector. The system consists of five laser beams distributed around the perimeter of the MVD support tube. There are five or six sensor positions along the support tube and one at either end attached to the CTD, from which the MVD is mounted. During regular operations the main purpose of the laser system will be to monitor gross movements of the MVD support structure with respect to the CTD in order to define stable periods for offline precision alignment using track data. However, the system proved its worth before and during the assembly of the MVD through 2000−01. Tests showed that the first design of the construction support frame was not rigid enough and needed strengthening. During assembly of the two halves of the MVD and their transport to DESY, periodic measurements were taken with the laser system to monitor any distortions in the MVD cylindrical support tubes. Measurements were also taken before and after the delicate operation to put the two halves together at DESY prior to a full test of the MVD using cosmic rays and finally after installation of the MVD in ZEUS. For the measurements up to and including the installation of the MVD, a prototype readout system with a limited number of channels was used. The final VME readout boards were completed in late 2001

and installed together with the online control system in January 2002. The system has been integrated into the MVD slow−control system and procedures are being developed for routine measurement and analysis of optical alignment data. Figure 2 shows the raw signals from all sensor positions along one of the five−laser beam lines.

Work has started on developing the tools needed for precision alignment using track data. A pattern recognition and fit program using CTD and MVD barrel data for through-going cosmic ray tracks, developed by our NIKHEF colleagues, is being used to study residuals at the level of individual wafers. This will then be extended to use the new general tracking software on selected classes of track data.

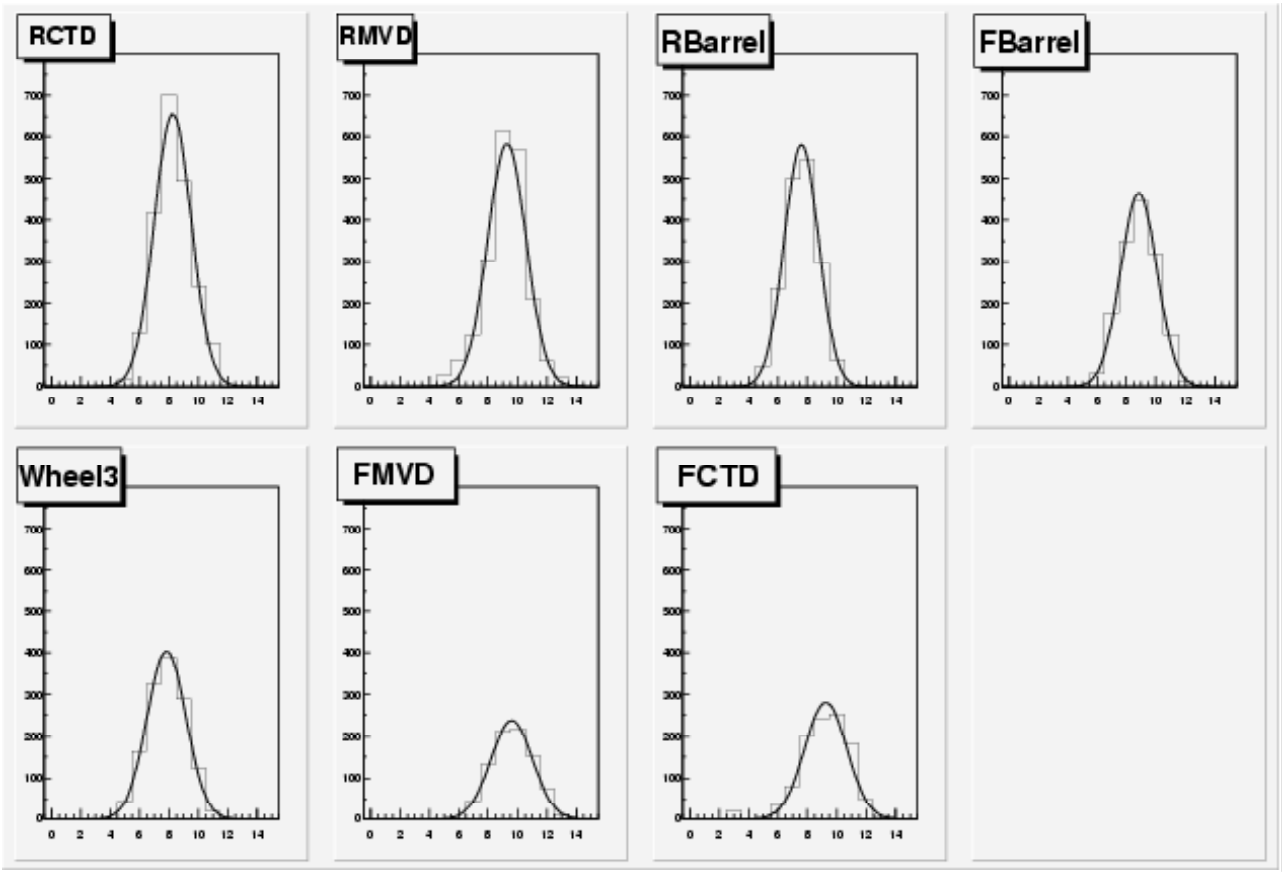

Figure 2: MVD optical alignment system. Signals from sensor positions along one laser beam. The positions labelled RCTD and FCTD are on flanges at the rear and front (wrt the proton beam) ends of the CTD respectively, the others are distributed along the MVD support tube. The curves are from simple gaussian fits to the signal profiles.

3.4 Installation

Installation was highly non−trivial because of space limitations and the delicate nature of the MVD. The procedures were worked out through extensive discussions with NIKHEF and DESY engineers and all the key stages were tested using various full−scale mock−ups. Apart from the challenge of getting the MVD into the central tube of the CTD with only mm clearance, the major problem was handling the 4m long readout and service cables attached to the MVD. These had to be fed in bundles through the CTD first. The installation scheme worked perfectly and the MVD was installed by 6 pm on 27th March 2001. The final part of the installation was arranging the cables between the MVD and patch boxes in the very limited space around the new rear combined function magnet. This turned out to be a classic problem of fitting a round object (cables around the

cylindrical magnet) into a square hole (aperture left when the ZEUS rear calorimeter is closed). Although the cable routes and clearances had been checked very carefully beforehand, the first attempt failed and the calorimeter could not be closed completely. It turned out that some drawings used in the planning had not been completely accurate. The UK team had a weekend in which to try again and by using a simple wooden former and a lot of hard work managed to persuade the cables to take a more rectangular profile thus allowing the calorimeter to close with a few mm to spare.

3.5 Global track trigger

The Global Track Trigger (GTT) is a new trigger component for ZEUS, which will eventually replace the function of the CTD SLT. It will combine the information from the (old) transputer based readout system used for both the CTD and STT with that from the (new) VME based readout system of the MVD. ZEUS−UK has responsibility for algorithm development and implementation. The GTT hardware consists of Gigabit ethernet communications and a farm of 12 1 GHz Linux PCs for processing. This augments the original CTD second level transputer based system: the farm hardware has been funded through the ZEUS Yale group. The GTT system for integrating CTD and MVD information is complete and has been tested within the ZEUS DAQ system. The STT readout has been added and data sizes are somewhat smaller than those from the CTD.

The algorithm for combining CTD and MVD information in the barrel region is being tested with the first real data. Work will begin shortly on integrating the STT and forward MVD information into the existing algorithm. The performance of the algorithm has been studied extensively, using Monte Carlo simulated events, trigger pass-through events taken during data taking last year, and cosmic muons taken during a short run in July this year.

To study the GTT latency before *ep* interaction data are available, a playback system was created. Monte Carlo events stored in memory are injected into the GTT trigger chain at the component VME interfaces, and sent through the GTT system exactly as for normal data. Using simulated high-E_T dijet photoproduction events containing both MVD and CTD data, at an input rate of 400 Hz, the deadtime was found to be 1.4%, consistent with the performance of the existing ZEUS DAQ and trigger systems during data taking at the end of 2000.

The resolution performance of the algorithm with simulated MVD data has been studied for track and event vertex parameter reconstruction. The event vertex resolutions for the reference Monte Carlo sample are summarised in Table 1. The resolution of the GTT using CTD-only information is significantly better than the existing CTD SLT due to the use of the stereo information rather than the z-by-timing data. The improvement in the z-resolution of the primary interaction vertex will help to reduce background considerably and is also a necessary first step for more sophisticated trigger calculations, such as event track impact parameter distributions and/or secondary vertex algorithms. At present the GTT (MVD + CTD) is operating in passive mode while the optimization of the HERA beam optics and luminosity continues.

3.6 Online software

The MVD run control, slow control and monitoring is carried out via a package based on the CERN Root software and known as 'Green'. This package includes histogramming and event display services and was written by ZEUS−UK staff. It has proved extremely flexible, and was used throughout the testing of the MVD. It is now fully integrated with the ZEUS global run control and is being used during data taking.

	σ_z(vertex) in mm
Current CTD−SLT	84.4
GTT (CTD only)	11.3
Current Offline (No MVD)	1.14
GTT	0.046

Table 1: Event Z−vertex resolution for GTT, existing CTD−SLT and existing offline reconstruction.

4 The HERA polarimeter upgrade

One of the most important objectives of the HERA II physics programme is the systematic study of the dependence of the neutral and charged current deep inelastic scattering cross sections on the polarisation of the lepton beam [2,3]. These measurements require a high degree of lepton−beam polarisation and excellent precision on the polarisation measurement (< 1%). For this purpose a polarimetry upgrade project was set up in 1999; the POL2000 project.

At HERA leptons become naturally transversely polarised through the emission of synchrotron radiation (lepton spin flips; Sokolov-Ternov effect). The lepton beam transverse polarisation is converted into longitudinal polarisation near the interaction points by spin rotators. The HERA ring polarisation is measured by two polarimeters: TPOL — the transverse polarimeter which measures transverse polarisation, located in the HERA-West area close to HERA-B; and the LPOL — the longitudinal polarimeter which measures longitudinal polarisation [4], located in the HERA-East area close to HERMES. The degree of polarisation is measured by scattering alternately right- and left-circularly polarised laser light off the polarised lepton beam. The back-scattered Compton photons that are produced are then detected by a calorimeter. The two polarimeters operate differently. Transverse polarisation is determined by measuring the vertical, up-down, asymmetry of the back-scattered photons on the TPOL calorimeter face, while longitudinal polarisation is determined by measuring the energy asymmetry in the LPOL calorimeter.

The TPOL calorimeter is separated horizontally into two halves. The energy sharing between the upper and lower halves is used to determine the impact position of the photon in the vertical direction. The up-down position asymmetry used to determine the polarisation relies on the conversion of the up-down energy asymmetry into a vertical position. This conversion is referred to as the 'η-y transformation'.

The dominant systematic errors in the polarisation measurement relate either to the linearity of the calorimeter energy response or to the precision with which the η-y transformation is known. To determine the η-y transformation precisely, in situ, during data-taking we have implemented a silicon-microstrip detector system. This system (shown schematically in figure 3) is composed of two 60×60 mm^2 silicon-microstrip detectors placed in front of the calorimeter and behind a 1 X_0 thick lead pre-radiator. The strip pitch of the detector measuring the vertical co-ordinate is 80 μm. A detector with a strip pitch of 120 μm and for which every second strip is read out is used to measure the horizontal coordinate. A high flux of photons enter the TPOL detector. The energy depositted by these photons gives a dose of ~5 Mrad per year over an area of only 0.1 mm^2. In order to identify and correct for the effects of differential radiation damage in the silicon-microsrip detector a scintillating fibre mounted on a precision stage has been installed between the silicon-detector planes and the pre-radiator. The fibre will be scanned periodically across

the face of the silicon detector in vertical steps of 2.5 μm and will allow differential radiation damage to be identified and corrected for.

The upgraded TPOL detector has been commissioned using test beams at DESY and at CERN. The test-beam data on the energy response of the calorimeter, the η-*y* transformation obtained from the silicon microstrip detector and the fibre position calibration are shown in Fig. 4. The results demonstrate that the required performance has been achieved. The system has been installed and commissioned in the HERA tunnel.

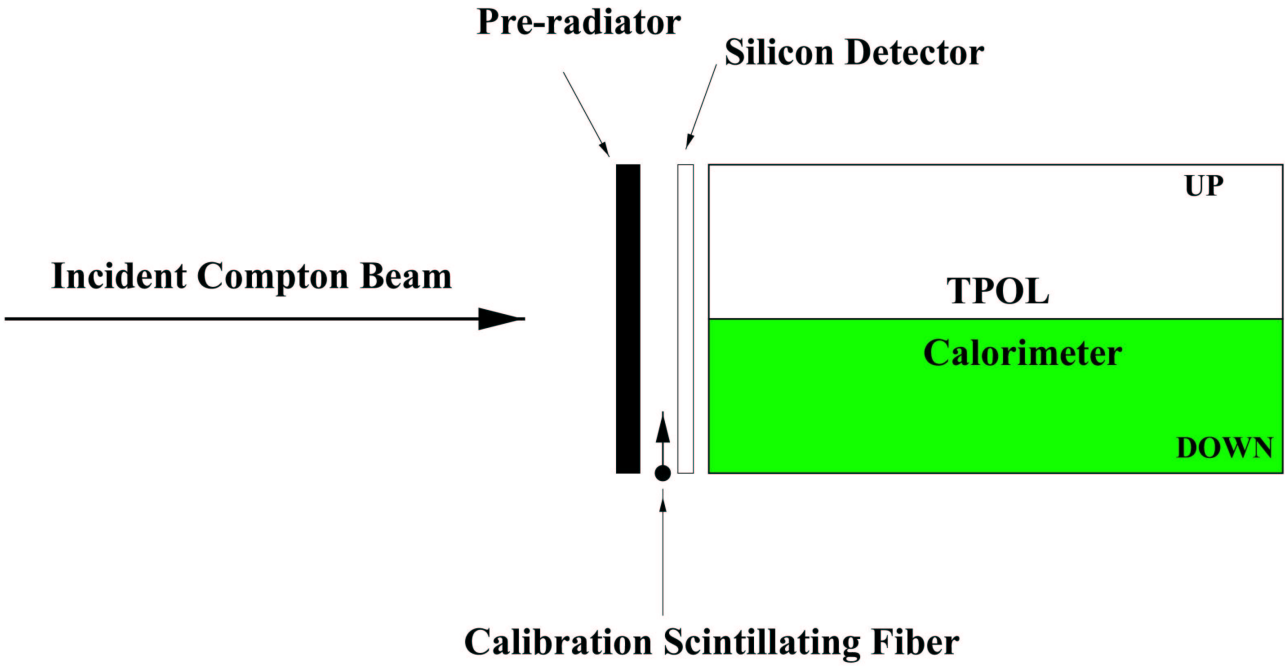

Figure 3: Schematic for the TPOL setup in the HERA tunnel, showing the 3 TPOL sub−detectors: calorimeter, silicon and fibre detectors. The pre−radiator is needed to convert the Compton photons. The calorimeter is divided into two independent halves. There are two silicon planes to measure the X,Y position of the Compton photon. The scintillating fibre detector is used for calibration and monitoring the silicon detector planes; the fibre is moved vertically by a precision stage.

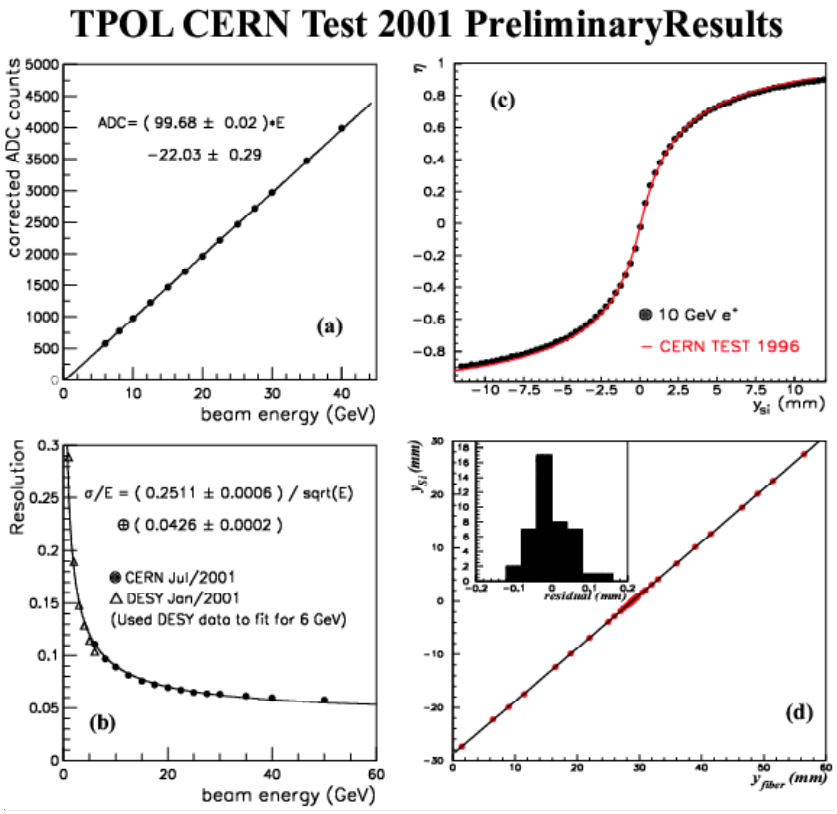

Figure 4: Summary of the DESY and CERN test beam results obtained during 2001. (a) The linearity of the TPOL calorimeter for positrons. (b) The calorimeter energy resolution obtained using both electron and positron beams. (c) The $\eta - y$ transformation for 10 GeV positron beam (dots). The solid line corresponds to the 1996 CERN test−beam result. (d) The $y-$coordinate reconstructed by the silicon for events with signals in the fiber versus the vertical position of the fiber, the insert shows the residuals to a straight line fit

5 Physics results

ZEUS-UK physicists are involved in a broad range of physics analyses. Very roughly, IC, Oxford and RAL are involved in structure functions and high-Q^2 studies, while Bristol, Glasgow and UCL cover the hadronic final states and heavy quark production.

5.1 Physics at high Q^2

5.1.1 High−Q^2 neutral current physics

In the Standard Model (SM), neutral current (NC) deep inelastic scattering (DIS) is described by the exchange of a photon or a virtual Z-boson between the incoming lepton and the proton. The Born level cross section for NC scattering is given by:

$$\frac{d^2\sigma_{\mathrm{NC}}^{e^{\pm}p}}{dxdQ^2} = \frac{2\pi\alpha^2}{xQ^4}\left[Y_+ F_2\left(x,Q^2\right) - y^2 F_L\left(x,Q^2\right) \mp Y_- xF_3\left(x,Q^2\right)\right]$$

where Q^2 is the negative of the 4-momentum transfer squared between the lepton and the proton, x is the Bjorken scaling variable, y is given by $Q^2 = sxy$ and $Y_\pm = 1 \pm (1\text{-}y)^2$. The parity violating structure function, xF_3, is expected to become significant at large Q^2.

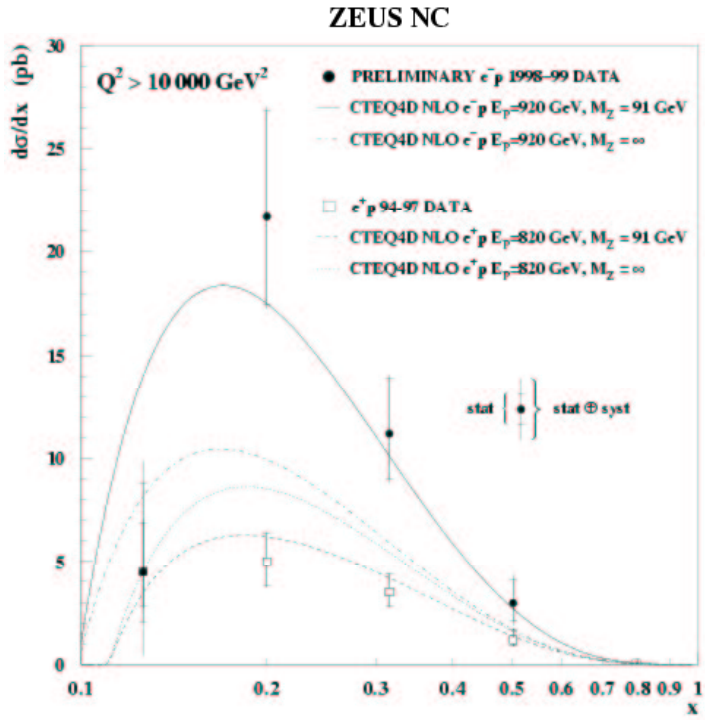

Figure 5: Comparison of measured differential cross sections $d\sigma/dx$ for e^-p and e^+p scattering as a function of x for $Q^2 > 10{,}000$ GeV^2. The curves show the Standard Model predictions.

ZEUS UK physicists have continued their leading role in studies of high-Q^2 physics at HERA. The determination of the NC cross section from the 16 pb^{-1} of e^-p data collected in 1998 and 1999 is in the final stages of the ZEUS editorial process [12] and the analysis of the 64 pb^{-1} of e^+p data collected in 1999 and 2000 is nearing completion. Figure 5 shows $d\sigma/dx$ for $Q^2 > 10{,}000$ GeV^2 for both e^+p and e^-p scattering along with the SM predictions. The e^-p cross section lies above the e^+p cross section and the SM prediction gives a good description of the data. Within the SM, the fact that the e^-p NC DIS cross section is larger than the e^+p cross section at high Q^2 is attributed to the fact that for e^-p NC DIS the interference between the photon- and the Z-exchange contribution is constructive while for e^+p NC DIS it is destructive. The reduced cross section, $\tilde{\sigma}$, where

$$\tilde{\sigma}^{e^\pm p}_{\mathrm{NC}} = \frac{1}{Y_+}\frac{xQ^4}{2\pi\alpha^2}\frac{d^2\sigma^{e^\pm p}_{\mathrm{NC}}}{dxdQ^2}$$

is shown at fixed x as a function of Q^2 in Fig. 6. For Q^2 values above ~3,000 GeV^2 the e^-p cross section lies above the e^+p cross section; consistent with the SM expectation.

Figure 7 shows the structure function xF_3 extracted by combining the e^-p data with the e^+p data collected in 1996 and 1997. The precision of the measurement is comparable with the first extraction of F_2 from the data taken in 1992. This measurement will benefit from the increased luminosity of HERA II. An improved measurement of xF_3 will impose a tighter constraint on the high-x valence quark distributions that play an important role in estimating very high-energy processes at the TEVATRON and at the LHC. In addition, the measurement of the dependence of the

neutral current cross sections on the charge and polarisation of the lepton beam will be sensitive to the electroweak couplings of the light quarks [5].

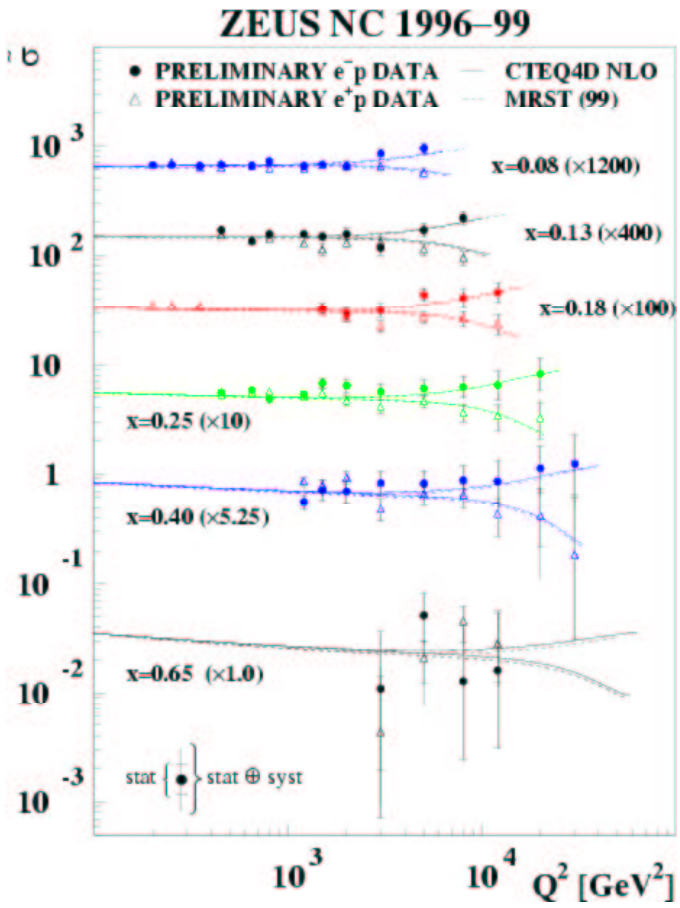

Figure 6: The reduced cross sections for e^-p (solid points) and e^+p (open squares) scattering as a function of Q^2, in bins of fixed x. Also shown are the Standard Model predictions.

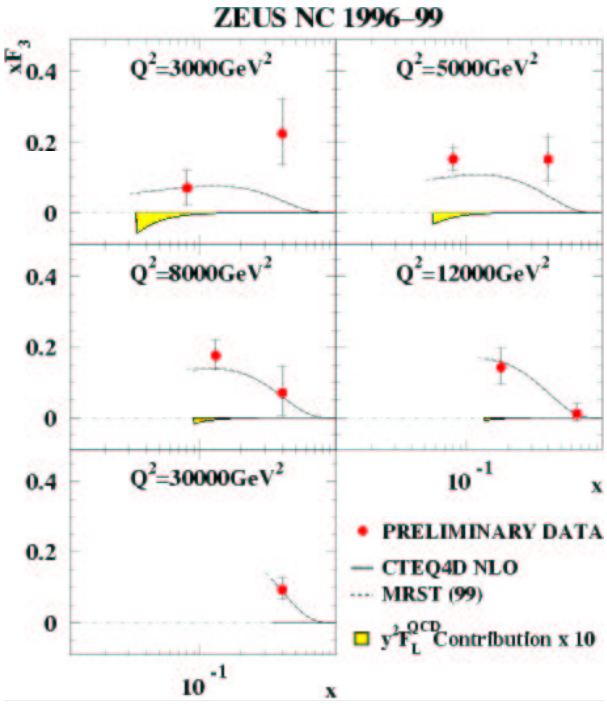

Figure 7: The strucure function xF_3 (solid points) as a function of x in bins of fixed Q^2. Also shown are the Standard Model predictions.

5.1.2 High−Q^2 charged current physics

In charged current (CC) deep inelastic scattering the exchanged *W*-boson picks out specific quark flavours from within the proton. Thus, e^+p CC DIS is sensitive to the *d*-valence quark density at high-*x* and the anti-*u* (and anti-c) quark density at low-*x*. In contrast, e^-p CC DIS is sensitive to the *u*-valence-quark density at high *x* and the anti-*d* (and anti-*s*) quark density at low *x*. Hence, by measuring the dependence of the CC DIS cross section on the charge of the lepton beam we are able to study flavour-specific parton densities directly.

The analysis of the e^-p data taken during 1998 and 1999 is now complete [13]. The analysis of the e^+p data taken in 1999 and 2000 is nearing completion and a publication is expected in the near future. Figure 8 shows the cross section $d\sigma/dQ^2$ for both e^-p and e^+p scattering. The e^-p cross section is higher than that of e^+p at all values of Q^2, rising to a factor greater than 10 at the highest Q^2 measured. In the quark parton model, this is understood to be due to the exchanged *W* coupling to the *u*-quark in e^-p scattering, while in e^+p scattering the *W* couples to *d*-quarks with a $(1-y)^2$ suppression. The Standard Model expectation, evaluated with the CTEQ5D parton density functions (PDFs), gives a good description of the data.

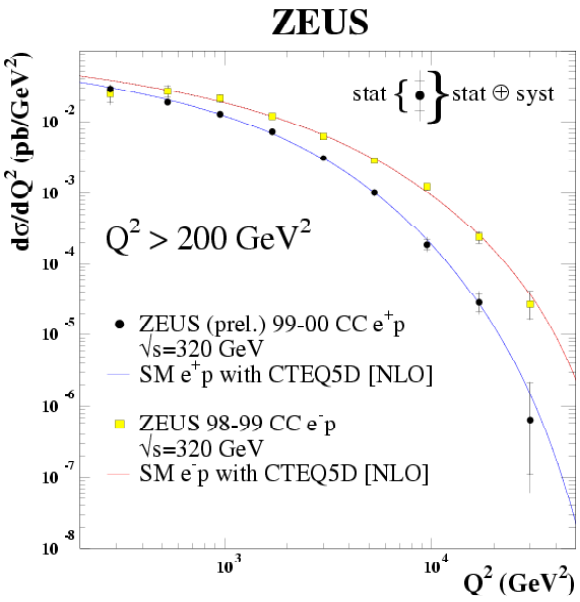

Figure 8: The CC DIS Born cross section, $d\sigma/dQ^2$, for e^-p data (squares) and e^+p data (filled circles). The dashed and solid lines show the Standard Model expectation evaluated using the CTEQ5D PDFs for e^-p and e^+p scattering, respectively.

The double differential CC cross section may be written as

$$\frac{d^2\sigma_{CC}^{e^\pm p}}{dxdQ^2} = \frac{G_F^2}{2\pi x}\left(\frac{M_W^2}{Q^2+M_W^2}\right)\tilde{\sigma}_{CC}^{e^\pm p}$$

where the e^-p reduced cross section, $\tilde{\sigma}_{CC}^{e^-p}$, is given at leading order in QCD by

$$\tilde{\sigma}_{CC}^{e^-p} = u + c + (1-y^2)(\bar{d}+\bar{s})$$

(for e^+p, change quarks to anti-quarks and vice versa). The reduced cross section, for e^-p, is plotted as a function of x at several fixed values of Q^2 in Fig. 9. The Standard Model gives a good description of the data. The precision of the measurements of the charged current cross section is statistically limited and will benefit greatly from the high luminosity running of HERA II. The addition of longitudinally polarised lepton beams will allow the polarisation dependence of charged current DIS to be studied.

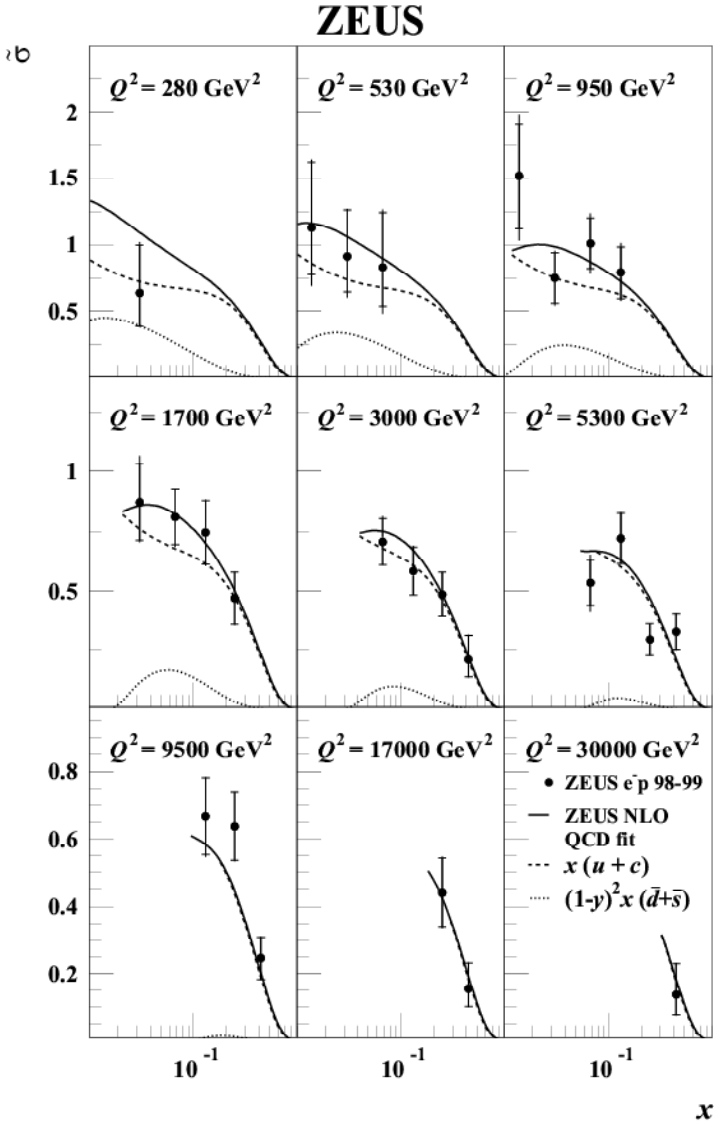

Figure 9: The reduced cross section, σ, as a function of x,for different values of Q^2. The points represent the data, while the expectation of the Standard Model evaluated using the ZEUS NLO QCD fit is shown as a solid line. The separate contributions of the PDF combinations $x(u+c)$ and $(1-y)^2x(d+s)$ are shown by the dashed and dotted lines, respectively.

5.2 NLO QCD fits

The UK has played a leading role in the interpretation of the data on the inclusive differential cross-sections by performing NLO QCD fits, using the DGLAP formalism, to determine the parton density functions (PDFs) and the strong coupling, α_S [6]. The standard (ZEUS-S) fit includes both the high-precision data on neutral current e^+p scattering [7] and fixed-target data. The PDFs extracted from the fit are shown in Fig. 10 and are compared to the MRST2001 [8] and CTEQ6 [9] PDFs.

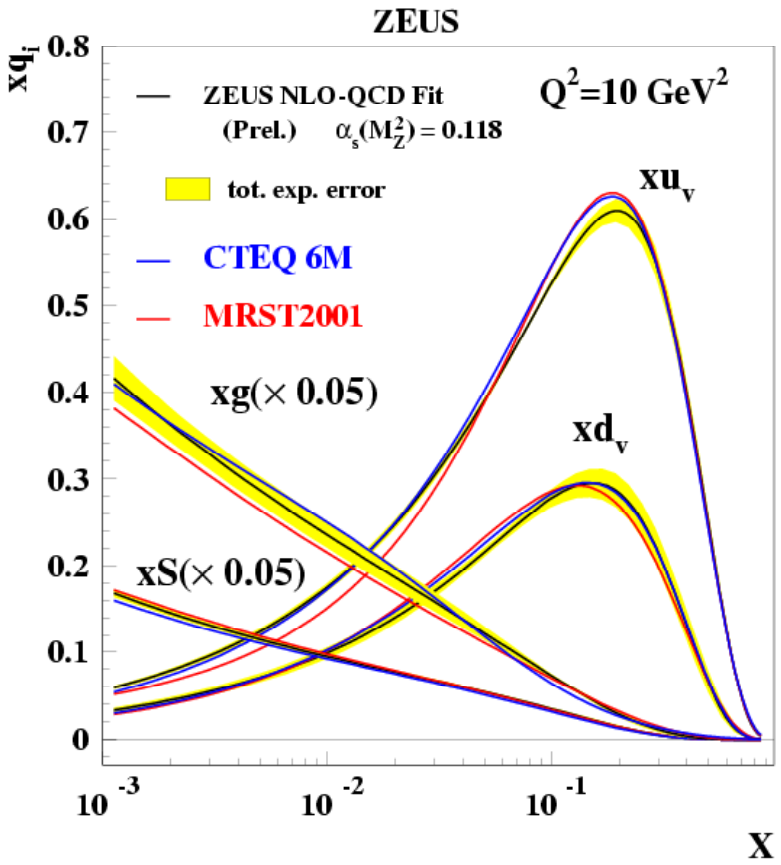

Figure 10: Comparison of parton distributions from the ZEUS−S NLO QCD fit to those from MRST2001 and CTEQ6. The error band shows the total experimental error from both correlated and uncorrelated sources.

A particular focus of this work has been the determination of the uncertainties on the parton distributions resulting from experimental sources. The error bands shown take full account of correlated experimental systematic uncertainties from all contributing data sets, including their normalisation uncertainties.

The ZEUS data are crucial for the determination of the gluon and the sea PDFs. These distributions are shown in Fig. 11. In this figure the additional uncertainty on these PDFs due to the variation of α_S is shown. This can be accounted for with full correlations to the PDF parameters by allowing α_S to be a parameter of the fit (ZEUS-α_S fit). The ZEUS-α_S fit also determines the value of α_S, leading to

$$\alpha_S = 0.1166 \pm 0.0008\,(\text{uncorr}) \pm 0.0032\,(\text{corr.}) \pm 0.0036\,(\text{norm.}) \pm 0.0018\,(\text{model})$$

where the four uncertainties arise from the following sources: statistical and other uncorrelated sources; correlated systematic sources from all contributing experiments excluding their normalisation uncertainties; normalisation uncertainties; model uncertainty. The model uncertainty arises from the variation of model inputs such as the value of Q_0^2 at which the input PDFs are parametrised, the form of the input parametrisation, the choice of data sets entering the fit, the kinematic cuts applied to these data sets and the choice of heavy quark production scheme. The PDF parameters are less sensitive to the model assumptions than α_S, thus it is clear that, within the theoretical framework of leading twist NLO QCD, the uncertainties due to model assumptions are not significant compared to the experimental uncertainties.

The NLO DGLAP formalism is expected to fail at low Q^2. The combination of the new precise fit analysis and the precise low Q^2 data [10] make it possible to quantify this expectation. In Fig. 12 the ZEUS-S fit is shown extrapolated

back into the kinematic region of the ZEUS BPT 1997 data. It is clear that the formalism is unable to describe the data for $Q^2 \leq 1$ GeV^2.

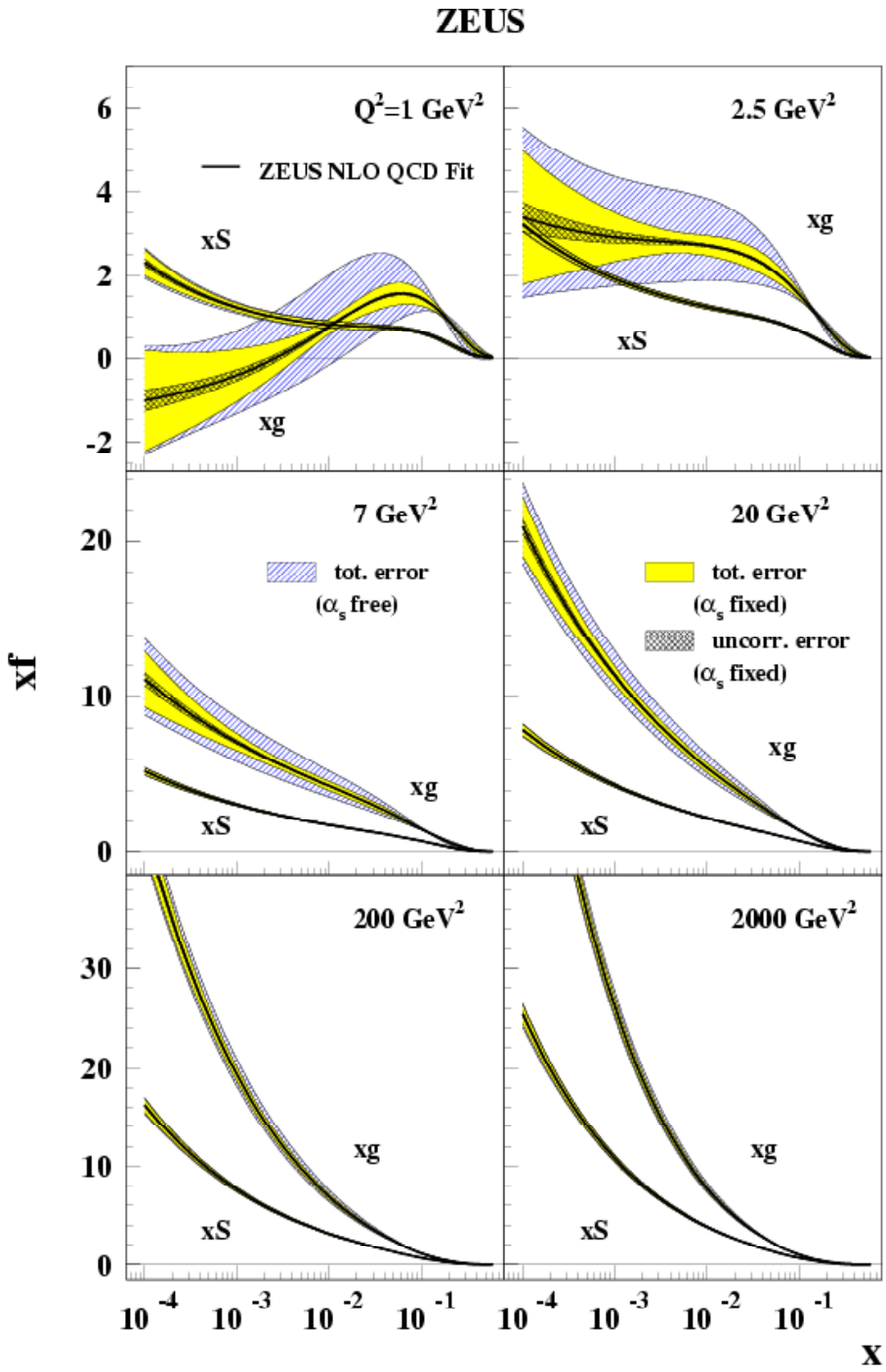

Figure 11: Comparison of gluon and sea distributions from the ZEUS−S NLO QCD fit for various Q^2. The cross−hatched error bands show statistical and other uncorrelated systematic uncertainties, the grey error bands show the total experimental uncertainty including correlated systematic uncertainties and the hatched error bands show the additional uncertainty coming from variation of the strong coupling constant, α_S.

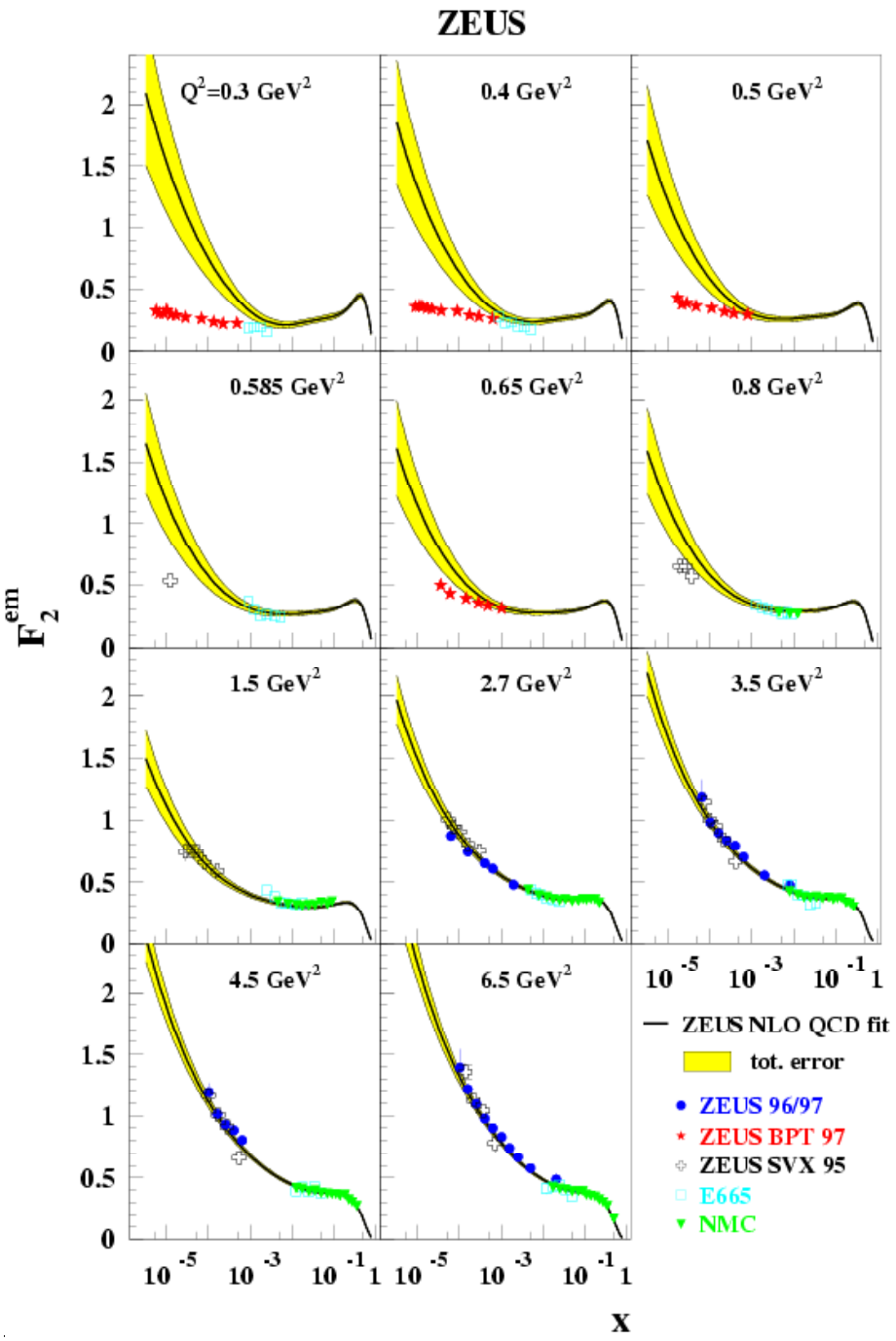

Figure 12: F_2 data at very low Q^2 compared to the backward extrapolated ZEUS−S NLO QCD fit. The error bands represent the total experimental error from both correlated and uncorrelated sources.

In the ZEUS-S fit, the valence PDFs are determined by the fixed target data, which suffer from uncertainties due to the need for heavy target corrections. However, a fit can be made to ZEUS data alone (ZEUS-O fit), if the high Q^2 e^+p data on the CC cross-section [11] and the e^-p data on the CC [13] and NC [12] cross-sections are included. When this ZEUS-O fit is done using only the published e^+p data, the level of precision with which the valence distributions can be measured is approximately half of that of the ZEUS-S fit. However, if the e^+p data from 99/00 [14] are also included, then the level of precision is considerably improved, as illustrated in Fig. 13. It is clear that the forthcoming high-luminosity running will allow us to extend significantly these studies.

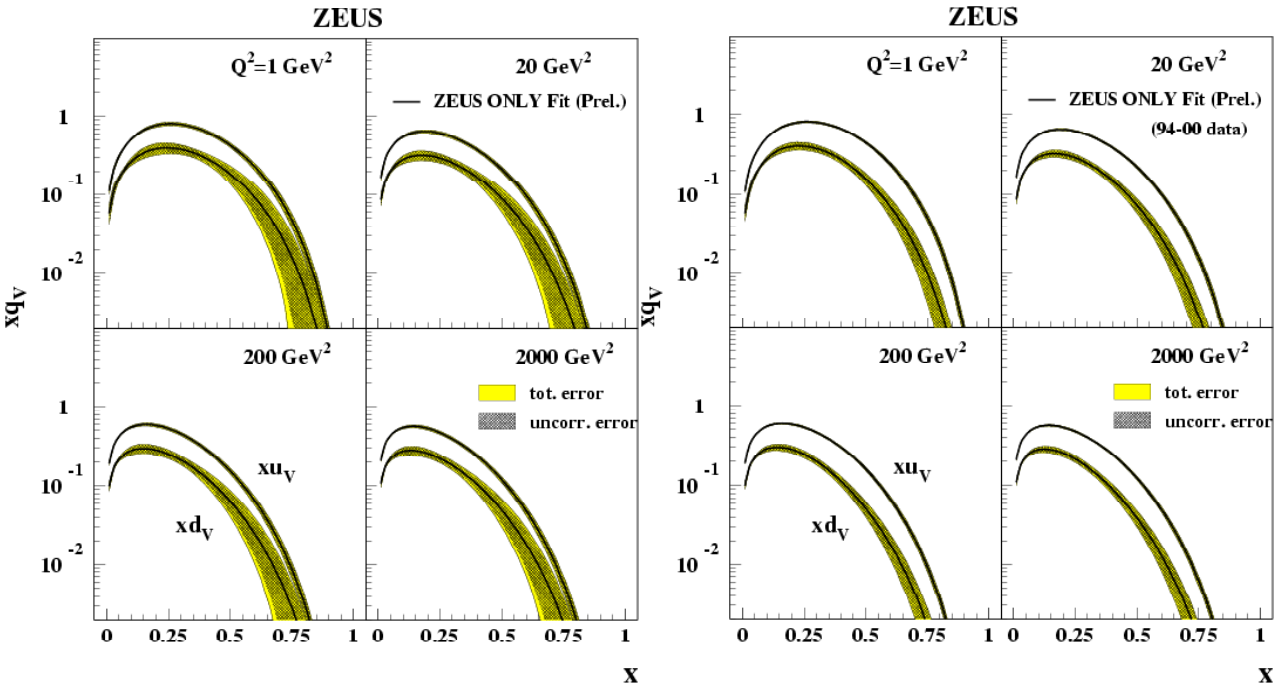

Figure 13: The xu_v and xd_v distributions from the ZEUS−O NLO QCD fit, using e^-p 98/99 data and e^+p 94/97 data (top), and using additional e^+p 99/00 data (bottom). The error bands show the uncertainty from statistical and other uncorrelated sources separately from the total uncertainty including correlated systematic uncertainties.

5.3 Heavy quark production

ZEUS UK groups have been involved in many aspects of the programme to understand heavy quark production. Analyses investigating the production mechanisms and rates for beauty and charm quarks are making significant contributions in a field that is still poorly understood. Precise measurements of charm in DIS and charm associated with jets in photoproduction are now being made. These measurements are discussed below along with the first measurement of open beauty production at ZEUS.

5.3.1 Charm production in DIS

Heavy quarks, particularly charm, are produced copiously in DIS, predominantly via the boson-gluon fusion process. This means that measurements of charm production allow, in principle, a direct determination of the gluon density in the proton. Charm has traditionally been identified using two decay chains, $D^{*+} \rightarrow D^0\pi^+$, $D^0 \rightarrow K^- \pi^+$ or $D^0 \rightarrow K^- \pi^- \pi^+\pi^+$. Each of these modes has a low background but also a small branching ratio. Using a luminosity of 37 pb^{-1}, ZEUS has published a measurement of charm production via these two decay modes [15]. Predictions of NLO QCD describe the data well over the full range in Q^2. The gluon distribution in the proton used was determined from fits to inclusive measurements of the proton structure function, F_2. The consistency of this prediction with the charm data demonstrates the universality of the gluon distribution in the proton, independent of the final state. Using all currently available ZEUS data along with other decay channels will greatly improve the precision of these measurements. UK physicists are taking a leading role in both of these directions. Very high-statistics measurements of heavy quark production in DIS will be a major goal with the new data to be collected with the upgraded HERA accelerator and ZEUS experiment.

5.3.2 Charm production with jets

With the larger data sample in the photoproduction regime ($Q^2 < 1$ GeV^2), charm production accompanied by jets is providing a detailed picture of many aspects of QCD and, in particular, the charm content of the photon. The first measurement of charm quarks inside jets was published in 1999 [16], with UK physicists as principal authors. The results showed for the first time that charm is produced copiously in resolved-photon events. Building on these results, resolved-photon processes have been studied further in order to understand whether the charm quark is an active parton in the photon or is only produced in the hard scatter.

In charm events in which two jets are produced, measurements of the angle, θ^*, between the jet-jet axis and beam direction in the dijet rest frame allow the dominant propagator in the hard scatter to be determined. Events in which the photon acts as a pointlike object (boson-gluon fusion) have a quark propagator; the cross section as a function of $|\cos\theta^*|$ is therefore $\propto(1-|\cos\theta^*|)^{-1}$. In contrast events with a gluon propagator have a cross section which is $\propto(1-|\cos\theta^*|)^{-2}$. If charm were not active in the photon, then charm in resolved-photon processes would only be produced via gluon-gluon fusion that has a quark as the propagator. Events enriched in direct- or resolved-photon processes can be selected by requiring $x_\gamma^{OBS} > 0.75$ and $x_\gamma^{OBS} < 0.75$ respectively; the variable x_γ^{OBS} is the fraction of the photon's momentum taking part in the production of the two jets of highest transverse energy. Figure 14 shows the measured $|\cos\theta^*|$ distribution in the two regions of x_γ^{OBS}. The measurement is based on a luminosity of 119 pb^{-1}, almost all of the available pre-upgrade data. For $x_\gamma^{OBS} > 0.7$, the data show a shallow rise consistent with events having a quark propagator, whereas for $x_\gamma^{OBS} < 0.75$, the data show a more rapid rise to high $|\cos\theta^*|$, consistent with the dominance of a gluon propagator. Resolved-photon events with a gluon propagator can only arise if the charm is active in the photon. The data is adequately described by predictions from the PYTHIA MC simulation and provides the strongest evidence so far of a heavy quark density in the photon.

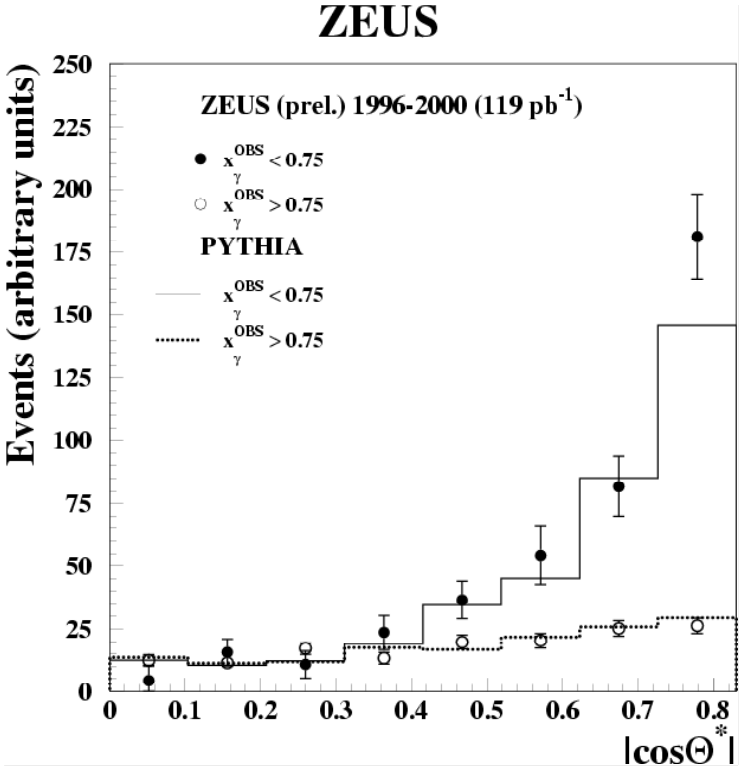

Figure 14: The $|\cos\theta^*|$ distribution in charm−tagged events for $x_\gamma^{OBS} > 0.75$ and $x_\gamma^{OBS} < 0.75$. Predictions from the PYTHIA MC are compared to the data.

Charm photoproduction has also been used to investigate the evolution of photon structure with virtuality, Q^2. This measurement also uses a luminosity of over 100 pb^{-1}. In inclusive dijet events the ratio, $\sigma(x_\gamma^{OBS}<0.75)/\sigma(x_\gamma^{OBS}>0.75)$ falls with Q^2, indicating the suppression of resolved-photon events with increasing photon virtuality. Figure 15 shows

the ratio $\sigma(x_\gamma^{OBS}<0.75)/\sigma(x_\gamma^{OBS}>0.75)$ for dijet events accompanied by a charm quark tagged by a reconstructed D^* meson. The data is compared to various leading order Monte Carlo models. In Fig. 15(a), models in which the partonic content of the photon is either suppressed or has no suppression as a function of Q^2 are compared to the data. Both models adequately describe the features of the measurement. Comparison of models with no explicit resolved-photon component with the data are made in Fig. 15(b). The AROMA model, which implements the DGLAP evolution scheme, lies below the data. The CASCADE model, which implements a version of the CCFM evolution scheme, gives a good description of the data.

The fact that the ratio does not change significantly with Q^2 in this range is in marked contrast to the case in which the charm requirement is not made and suggests that the suppression of the low-x_γ^{OBS} cross section due to charm and the suppression due to photon virtuality are not independent. This has been quantified by extrapolating the measurement to the full kinematic range of the $D^{*\pm}$ meson. The result is shown in Fig. 15(c) and demonstrates that the ratio falls off more slowly in the presence of charm than it does when charm is not required.

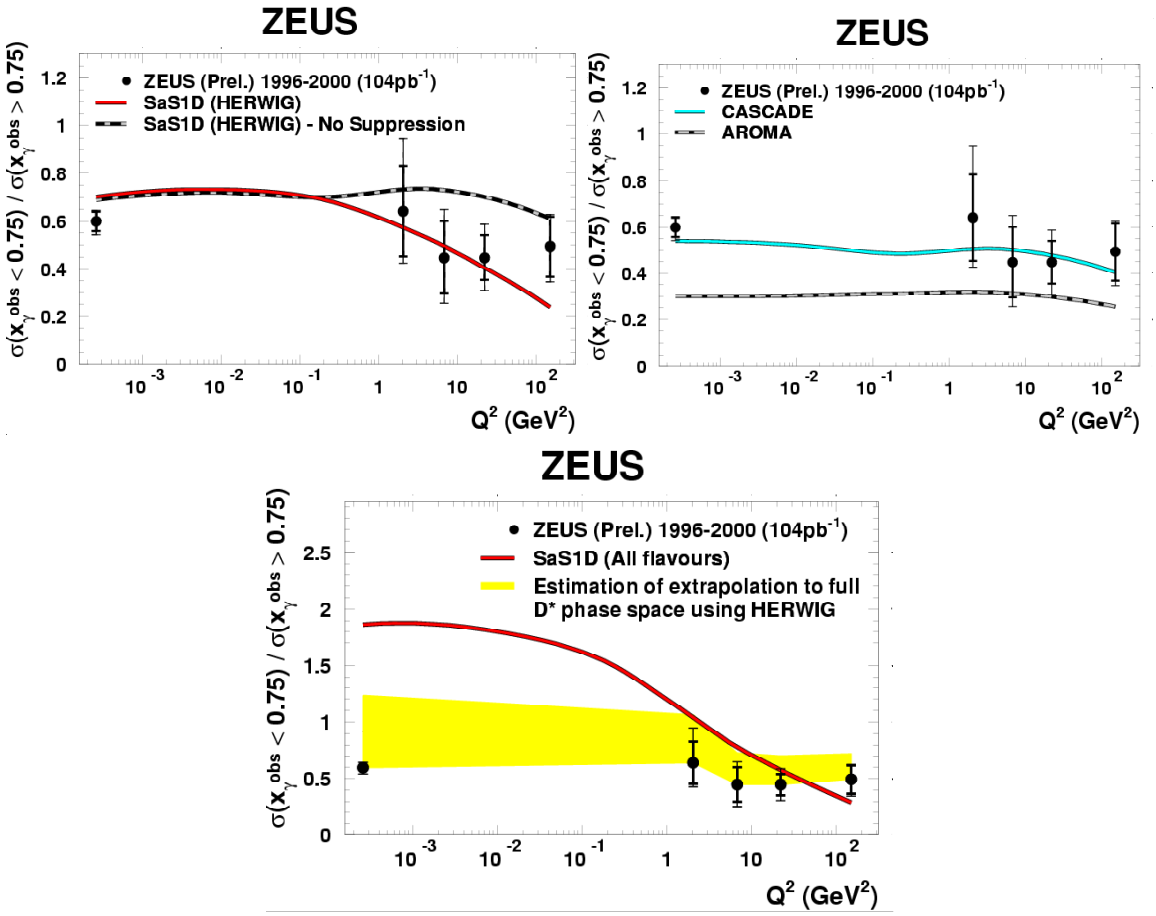

Figure 15: Ratio of low to high x_γ^{OBS} for events with a D meson compared to (a) the SaS1D photon structure functions, (b) the Aroma and Cascade MC models. In (c), the data is extrapolated to the full phase space of the D* meson and compared to the SaS1D photon structure function.*

5.3.3 Beauty production

Beauty production can be detected by identifying electrons produced in the semi-leptonic decay of the B meson. UK physicists have used the specific energy loss of electrons, measured in the CTD, to obtain evidence for beauty production. Measuring the transverse momentum of the electron relative to the jet axis (p_T^{rel}) identifies the beauty component. Electrons from beauty decays are expected to have a harder p_T^{rel} spectrum owing to the mass of the b

quark, as can be seen in Fig. 16. The beauty fraction has been extracted by fitting the data distribution. The measurement was published in 2001 [17].

Existing measurements of open beauty production from HERA, $\gamma\gamma$ collisions at LEP and proton-anti-proton colliders show cross sections that are high when compared to standard NLO QCD predictions. A direct comparison of the ZEUS result with a NLO QCD prediction has also been performed. The result, shown in Fig. 17, also lies above the theoretical prediction.

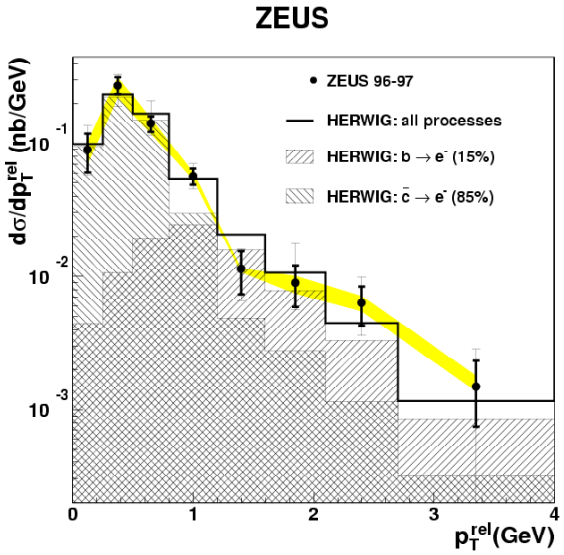

Figure 16: The transverse momentum of the electron relative to the jet axis, showing the presence of beauty quarks

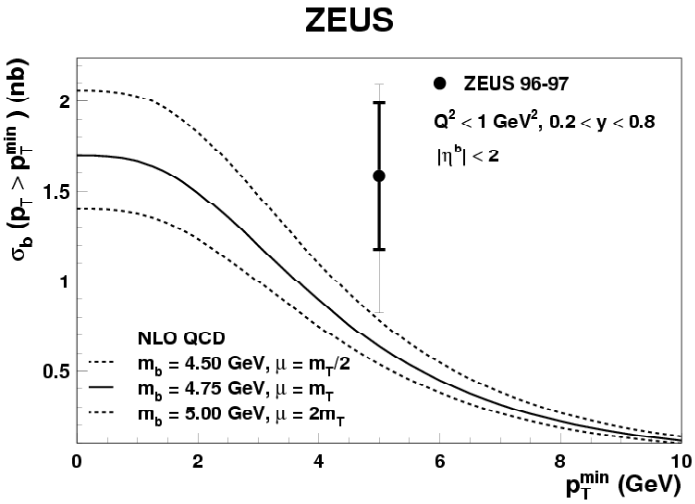

Figure 17: Extrapolated beauty quark cross section compared to NLO QCD predictions.

The presence of heavy quarks in the evolution of the photon structure offers a promising window for understanding the development of QCD structure, splitting functions and threshold effects. The ability at HERA to select concurrently on jet transverse energy, E_T^{jet}, photon virtuality and x_γ^{OBS}, as well as to compare heavy flavour jets with untagged jets, makes it uniquely suitable for detailed studies in this area. Thus, heavy-flavour jet production will be of increasing importance in the physics of HERA II.

5.3.4 Charm Production in Diffractive Scattering

The study of charm production in diffractive scattering is a crucial part of the investigation of the diffractive process and the underlying mechanism responsible for diffraction. This is because charm production occurs predominantly in gluon-driven interactions. The analysis of charm in diffraction has been performed by reconstructing $D^{*\pm}(2010)$ mesons in diffractive interactions. Members of the UK group and has been submitted to Physics Letters. B. The high luminosity of HERA II combined with the enhanced charm tagging capability of the ZEUS MVD will allow the definitive measurement of charm production in diffraction.

5.4 QCD and the hadronic final state

5.4.1 Event shapes

A recent revival of interest in the study of event shape measurements has been prompted by theoretical developments in the understanding of hadronisation or power corrections. Power corrections allow perturbative QCD calculations to be extended into the region of low momentum transfers using approximations to higher−order graphs. At HERA, the Q^2 scale can be varied over four orders of magnitude enabling power corrections (proportional to $1/Q^n$) to be studied in detail. The data are compared to theoretical expectations for the power corrections and the effective coupling α_0 (μ_I), specified at the infra−red matching scale $\mu_I \cong 2$ GeV, and $\alpha_S(M_Z)$ are extracted.

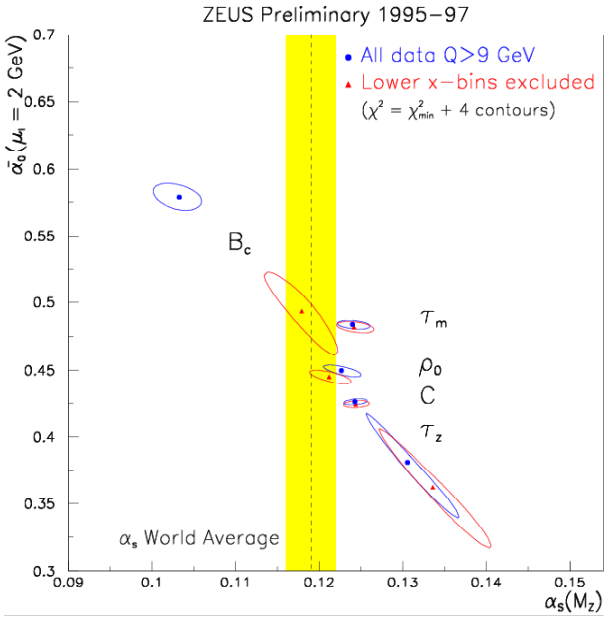

Figure 18: ZEUS preliminary contour plot of two−parameter fits of α_0 (μ_I) and $\alpha_S(M_Z)$ to mean event shape variables. Two σ statistical−uncertainty contours for fits both including and excluding the lower x data for τ, B, τ_C, ρ and C parameters are indicated.

In the Breit frame, where the exchanged gauge boson in DIS is purely space-like, the incoming quark is back-scattered with equal and opposite momentum ($Q/2$). Event shapes have been measured in the direction of the struck quark, corresponding to the current region, which is directly analogous to one hemisphere of a purely time-like e^+e^- interaction. Several event shape variables have been studied which have varying sensitivity to hadronisation/power corrections. Thrust, ($\tau = 1 - T_z$), and jet broadening (B) sum the longitudinal and transverse momenta, respectively, of individual particles along the photon axis. Thrust, τ_c, is also defined with respect to the reconstructed thrust axis, in order to compare directly with data from e^+e^- annihilation. Jet mass (ρ) and the C parameter sum the product of two particle momenta weighted by $1-\cos\theta_{ij}$ and $\sin^2\theta_{ij}$, respectively. These variables are each measured in the current

region of the Breit frame and are scaled by the total visible energy (E_{vis}). Mean values of these event shapes have been measured by ZEUS [18] and can be interpreted theoretically via

$$\langle F \rangle = \langle F \rangle^{\text{pert}} + \langle F \rangle^{\text{pow}}$$

where

$$\langle F \rangle^{\text{pert}} = C_{1,F}\,\alpha_S(Q) + C_{2,F}\,\alpha_S^2(Q)$$

with C_{1F} and C_{2F} being perturbatively calculable coefficients determined by the DISENT NLO program. The power corrections are proportional to $1/Q$ with

$$\langle F \rangle^{\text{pow}} = M' \frac{\alpha_F}{Q} \frac{16\mu_I}{3\pi} \left[\alpha_0(\mu_I) - \alpha_S(Q) - \frac{23}{6\pi}\left(\ln \frac{Q}{\mu_I} \right) + 1.45\alpha_S^2(Q) \right]$$

Here α_F is a calculable, F-dependent, coefficient and $M' = 2M/\pi \cong 0.95$ is a two-loop level refinement to the calculations called the Milan factor.

Using the NLO calculation plus power correction approach described above, the mean event shape values versus Q is measured. Overall, a reasonable description of the data can be achieved, although the x-dependence of variables measured with respect to the photon axis, τ and B, is not well described. The major theoretical uncertainty is that due to the renormalisation scale. The results of two-parameter fits to the ZEUS data both including and excluding the data at low x are shown in Fig. 18. The correlation of $\alpha_0(\mu_I)$ and $\alpha_S(M_Z)$ is high and negative for $\langle\tau\rangle$ but is less significant for other event shape variables. In each case, the data for the means of τ, B, τ_C, C and ρ are described reasonably well by the theory with a value of the universal non-perturbative parameter $\alpha_0(\mu_I)$ of $\approx 0.5 \pm 0.2$ and a value of $\alpha_S(M_Z)$ close to the world average. There are, however, theoretical uncertainties due to uncalculated higher-order x-dependent terms which appear to be especially significant for B. Ongoing refinements will generate further insight into non-perturbative QCD mechanisms in the generation of hadronic final states at high energies. This analysis is currently in the final stages of the ZEUS editorial process and will lead to a publication soon.

5.4.2 Jet production

Our studies of jets in photon-proton collisions at HERA continue to give information on the hadronic "structure" of the photon. The UK groups continue to lead these analyses. In the last report we presented our measurement [19] of the dynamics of three jet production with higher statistics than our previous measurement [20], showing explicitly the effects of the colour of the incoming quarks and gluons; a fundamental test of the strong interaction. In addition we have recently published [21] precise data on dijet photoproduction (see Fig. 19) at high E_T^{jet}. This publication included the dijet angular distributions.

Although these angular distributions present a reassuring picture of jet photoproduction in that the dynamics are well described by QCD, there is growing evidence for a significant discrepancy in the rate of resolved photon interactions, with the data lying above the NLO QCD expectations by around 30%. We have measured cross sections differentially in η_T^{jet}, E_T^{jet} and x_γ^{OBS}. None of the current parameterisations of the structure of the photon, convoluted with the NLO matrix elements, fully describe all features of the data. There is agreement with theory at high x_γ^{OBS} and high transverse energy, where the dependence on the photon structure is small. This represents a consistency check on the gluon distribution in the proton extracted from deep inelastic scattering. The data at low x_γ^{OBS} significantly constrain the parton densities in the photon in a region inaccessible at LEP; future parameterisations of the photon PDFs must take them into account.

On the other hand, the cross-section as a function of the cut on the transverse energy of the sub-leading jet (Fig. 19) suggests that the contribution from higher order processes may still be significant. The constraints imposed here on the parton densities in the photon would be made more stringent if improved higher-order or resummed calculations were available.

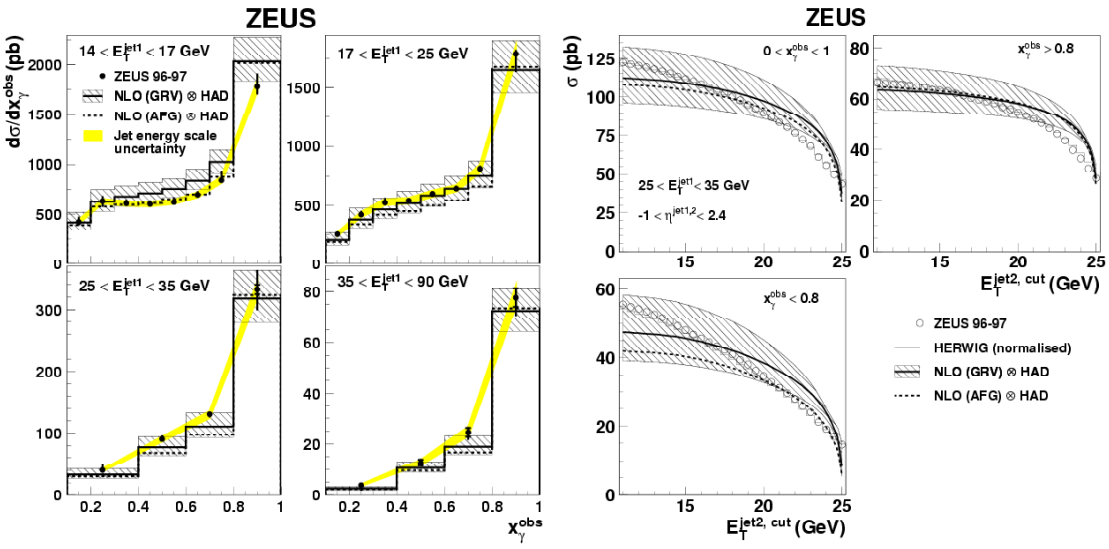

Figure 19: Left; ZEUS jet cross sections compared to the NLO QCD calculation of Frixione and Ridolfi. Right; total ZEUS dijet cross−sections for differing E_T cut on the sub−leading jet compared to HERWIG and the NLO QCD calculation. The shaded areas for the data and theory prediction indicate the hadronic energy−scale uncertainty and the theoretical uncertainty respectively.

We are seeking to expand our understanding of the QCD sub-process at even higher orders by studying the inclusive four-jet final state. The measurement of four-jet events is sensitive to multi-parton interactions. After selection of four-jet events, the two jets with the lowest invariant mass are combined. The angle between the leading jet in the resulting pseudo three-jet system, θ_3, is then determined. The distribution of $\cos\theta_3$ is shown in Fig. 20. The data rises towards the forward (proton) direction. Comparison with Monte Carlo models which do not include the effect of multiple interactions (Fig. 20a) do not provide a good description of the measured distribution. A Monte Carlo model that includes a soft underlying event also fails to describe the data. Models that include parametrisations of multi-parton interactions (Fig. 20b) provide a reasonable description of the data. The angular distribution for those events with high four-jet invariant mass, $M_{4\text{jet}} > 50$ GeV^2, is shown in Fig. 20c. Here models both with and without multi-parton interactions are similar and provide an adequate description of the data.

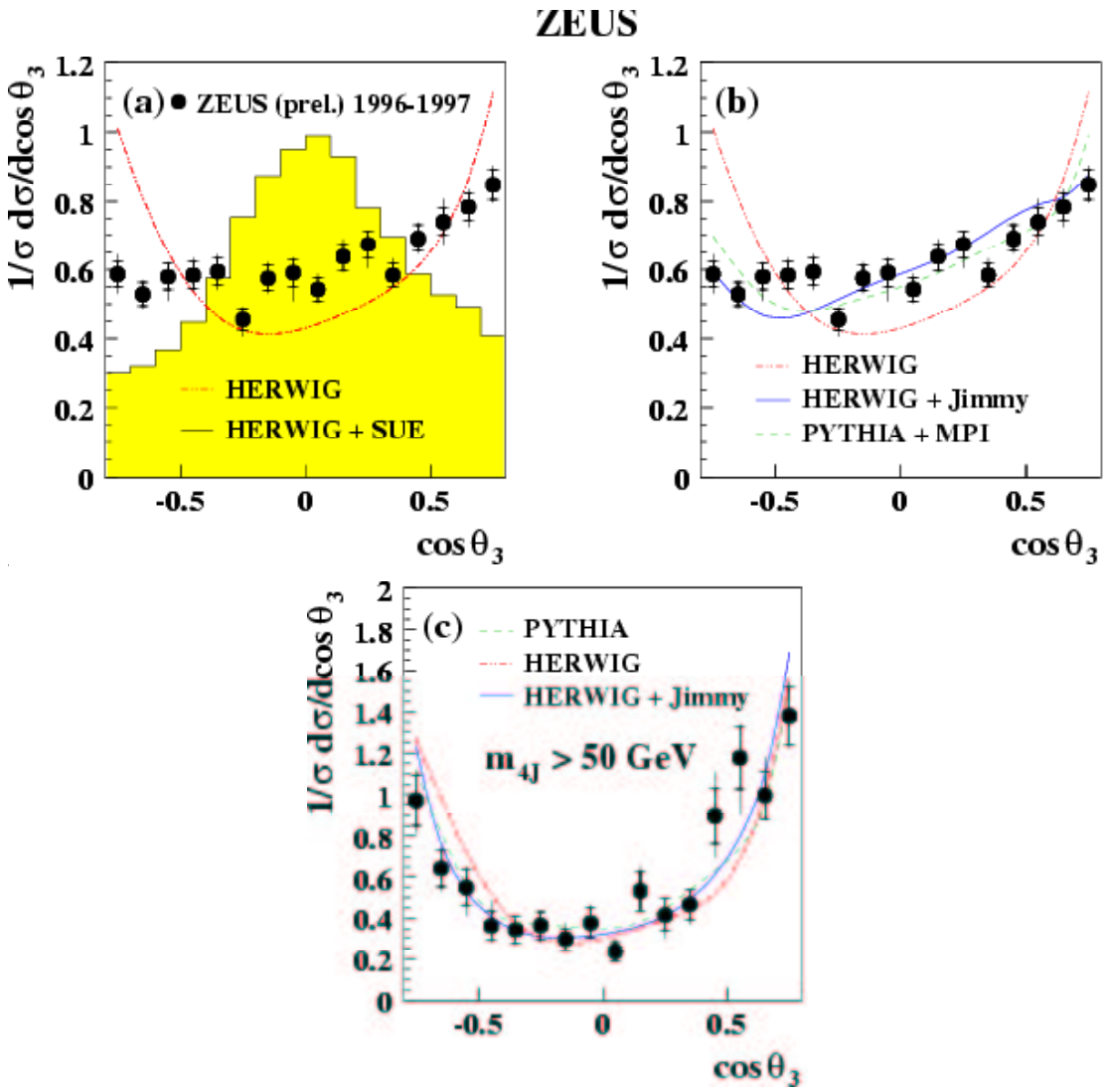

Figure 20: Four jet photoproduction: a) The angluar distribution of the pseudo three−jet system compared to standard HERWIG and a model including a soft−underlying event; b) HERWIG and PYTHIA models including multiparton interactions; c) the angular distribution with and without multi−parton interaction models for events with four−jet invariant mass, $M_{4jet} > 50\ GeV^2$.

5.4.3 Jet substructure

An important aspect of the description of the QCD final state in jet production is in the description of the structure of the jets themselves. To study this we have measured the topology of jets in photoproduction. The mean jet-shape can be studied by measuring the fraction of the jet energy contained within an η-ϕ cone of radius R to the full jet energy contained within a cone of radius $R = 1$. A second measure is afforded by counting the number of subjets within the jet for a varying distance scale, y_{cut}, used in the jet finding. The width of jets in QCD is sensitive both to the QCD coupling, α_S, and to the fragmentation of the parton that initiates the jet. The tendency for gluon initiated jets to be broader than quark initiated jets can be used to divide the sample into gluon enhanced (thick) and quark enhanced (thin) jets and to study the dynamics of the underlying sub-process. Figure 21 shows the dijet angular distribution in the dijet centre-of-mass frame for samples enriched in gluon-gluon, quark-quark and gluon-quark jets.

In addition, by studying the behaviour of the mean jet shape as a function of the jet transverse energy the QCD coupling constant can be extracted. Such a measurement is complimentary to that obtained from the study the jet rates themselves. A summary of the various measurements of α_S performed at HERA is shown in Fig. 22. The values

of α_S obtained from the study of jet shapes and subjet multiplicity are in agreement with the other measurements, providing a non-trivial test of the consistency of our understanding of the hadronic final state.

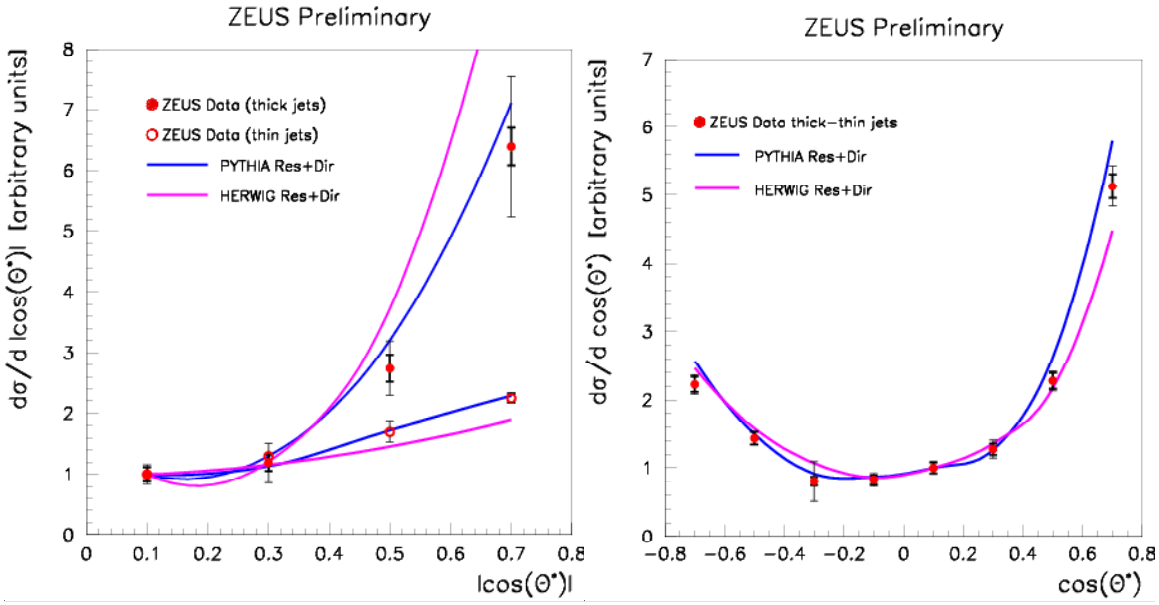

Figure 21: ZEUS preliminary jet cross−sections versus cosθ compared to HERWIG and PYTHIA.*

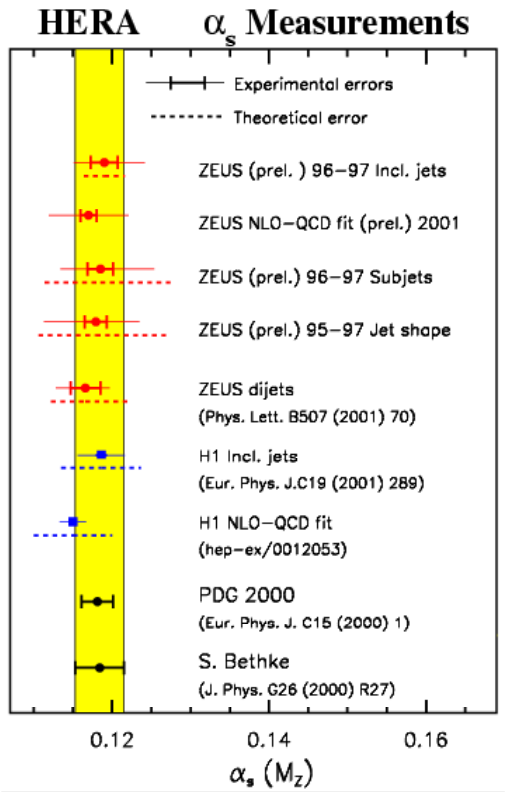

Figure 22: Summary of α_S determinations at HERA.

5.4.4 Virtual−photon structure

Both the behaviour of the pointlike virtual photon at high Q^2 and the hadronic structure of the low virtuality photon have been studied. By measuring dijet production as a function of the photon virtuality from very low, to very high Q^2, we were able to study the hadronic structure of the virtual photon. Building on our previous analysis [22], we have made use of the higher luminosity now available to study the virtual photon structure differentially in photon virtuality,

mean dijet transverse energy squared and x_γ^{OBS}. The result is presented in Fig. 23 and compared to the predictions of QCD evaluated using the SaS 1D [23] parametrisation of the virtual photon parton density functions.

As expected, the low-x_γ^{OBS} cross section falls more quickly with increasing Q^2 than the high-x_γ^{OBS} cross section and for $Q^2 > E_T^2$, the data is well described by the Monte Carlo with no resolved contribution being required. However, for $Q^2 < E_T^2$, the direct contribution alone is not sufficient to describe the data and further, the low-x_γ^{OBS} cross section is not well described by the Monte Carlo at lower Q^2.

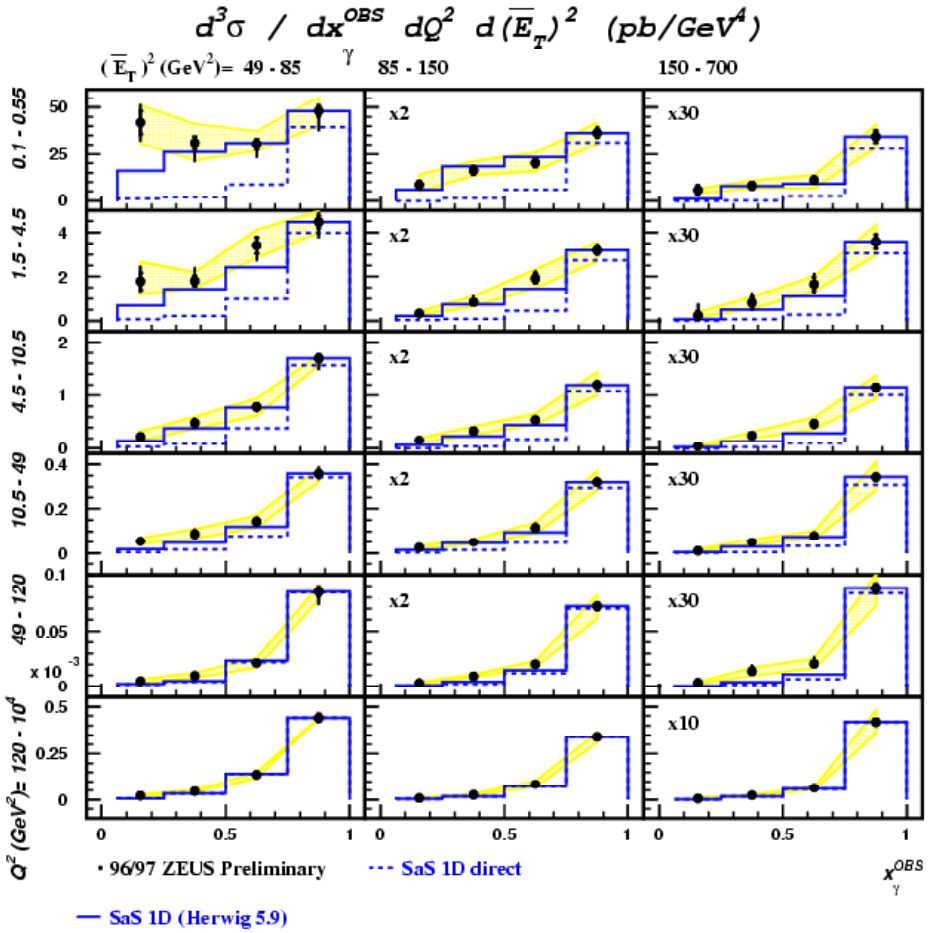

Figure 23: ZEUS preliminary dijet cross−sections, triply differential in Q^2, mean jet transverse energy squared and x_γ^{OBS} compared to HERWIG.

5.4.5 Strange hadron production

Strange particle production at HERA provides an important environment for the study of the hadron production mechanism in processes containing hadronic remnants and can yield important information on the universality of strange particle fragmentation functions. By considering strange particle production in conjunction with the production of high-E_T jets in the hadronic final state it is possible to study the dependence of the hadronisation mechanism on the underlying kinematics of the perturbative QCD sub-process.

Using the large event sample now available at ZEUS we have measured [24] strange particle production both to higher precision, and more differentially than before. The cross-section for K_S production in events with at least two jets with high-transverse-energy is reasonably well described in shape by available Monte Carlo models. Figure 24 shows that while the K_S and Λ cross section is reasonably well described in shape, normalising the overall Monte Carlo cross section to that given by the K_S data over estimates the rate of Λ baryon production with respect to K_S hadrons for HERWIG and slightly underestimates it for PYTHIA.

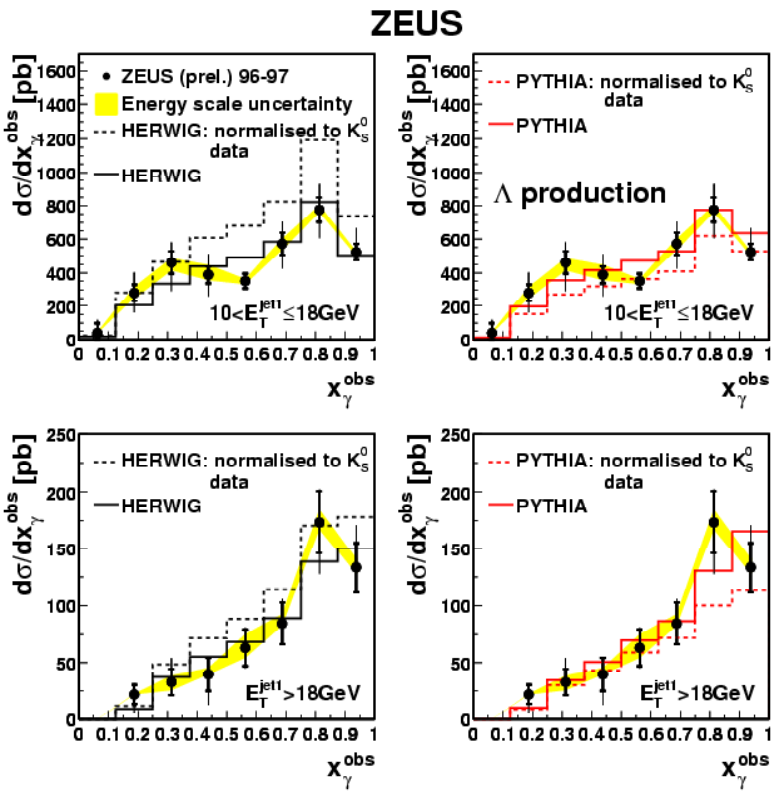

Figure 24: ZEUS preliminary cross−sections on Λ production for high transverse energy dijet photoproduction normalised both to the Λ data (solid) and to the K_S^0 data (dashed).

5.4.6 Prompt Photon Photoproduction

Further progress has been made in studying photoproduction processes in which a high-E_T photon is emitted. Such photons may be produced directly as part of the QCD hard scattering sub-process and are known as prompt photons. In a first ZEUS paper [25] the observation of such processes was confirmed at HERA and the basic characteristics of events with a prompt photon and a counterbalancing jet were established. In a more recent paper [26] the properties of inclusive prompt photons have been studied in more detail.

High energy photon production can be described as a sum of direct processes, dominated by the scattering of the incoming photon off a quark in the proton, and resolved processes, in which the incoming photon is a source of partons which subsequently scatter. Another source of photons comes from dijet processes in which a final state quark radiates a photon, referred to as radiative events. The requirement that the final-state photon be relatively isolated from other final-state particles reduces the radiative contribution and also neutral-meson backgrounds. The latter are subtracted by means of signal-shape properties as measured in the ZEUS barrel calorimeter. Figure 25 shows the effective transverse momentum of quarks within a proton, as they take part in direct photoproduction of a high transverse momentum prompt photon and a jet. Comparison is made with a variety of measurements from other experiments over a wide range of interaction energies, W. A consistent trend is observed. We are currently extending this analysis to include the study of prompt photons in DIS events. This entire area of study will be further enhanced by the very much improved luminosities available after the HERA upgrade.

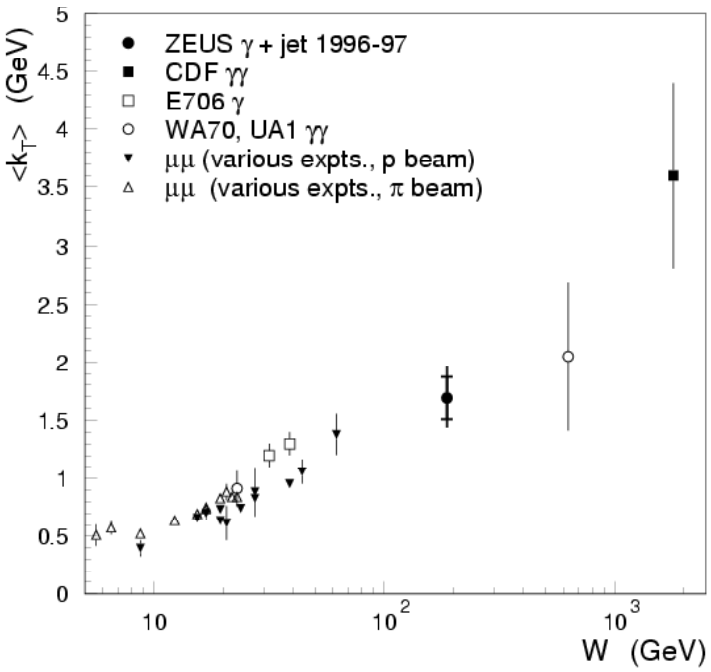

Figure 25: Effective transverse momentum of quarks within a proton, as they take part in direct photoproduction of a high transverse momentum prompt photon and a jet.

5.4.7 Isolated High−p_t Leptons and Searches for Heavy Resonances

Using data corresponding to an integrated luminosity of about 130 pb^{-1} (113 pb^{-1} of e^+p and 16.3 pb^{-1} of e$^-$ p), a search for resonances in the e$^{\pm}$(ν)−jet invariant mass spectrum from the reaction $e^{\pm}p \rightarrow$ e(νX) at a centre-of-mass energy of up to 318 GeV has been performed. No evidence for a resonance was found, so limits were derived for the production of leptoquarks. Limits vary with different leptoquark type and coupling, but extend for some coupling to masses above the HERA centre of mass energy.

The same data sample was used to select events with transverse momentum as measured in the calorimeter, P_t, greater than 20 GeV and the presence of a track with transverse momentum, p_t, greater than 10 GeV. In 17 events a well-isolated track was found. All of the 17 well-isolated tracks were identified as leptons: 10 were identified as electrons or positrons and 7 were identified as muons. The expected number of events from the SM processes was 11±1.6 electron-type and 5.4±0.7 muon-type events. The agreement with the SM was also good when, in addition, large transverse momentum (25 or 40 GeV/c) of the hadronic system was required. This is in contradiction to an excess of such events reported by H1 collaboration.

A search for single top production, $ep \rightarrow etX$, has been made. The SM prediction gives no measurable event rate but some models beyond the SM predict anomalous effective couplings of the type tuV or tcV ($V = \gamma, Z$) which could give rise to experimental signatures. The top decays predominantly to Wb. A search for W boson was made in the leptonic decay mode using the data sample described above and for the hadronic decay mode by selecting events with at least three jets. No deviation from the SM prediction was found. Limits on the FCNC coupling $k_{tu,\gamma}$ have been obtained.

Our recently published results [27] on dijet production at very high invariant mass, with higher precision than previously measured, allow the search for heavy resonances and new physics in the hadronic channel. Limits on $W^{\pm}$ and Z production in the final state have been obtained and are $\sigma_{e^+p\rightarrow e^+ZX} < 5.9\,\text{pb}$ and $\sigma_{e^+p\rightarrow e^+W^{\pm}X} < 7.4\,\text{pb}$ respectively. The Z limit is the first at HERA. Limits on the production of new heavy

resonances, *P*, coupling preferentially to the photon-gluon initial state, such as technicolour pseudo-Goldstone bosons [28], have also been obtained and are illustrated in Fig. 26.

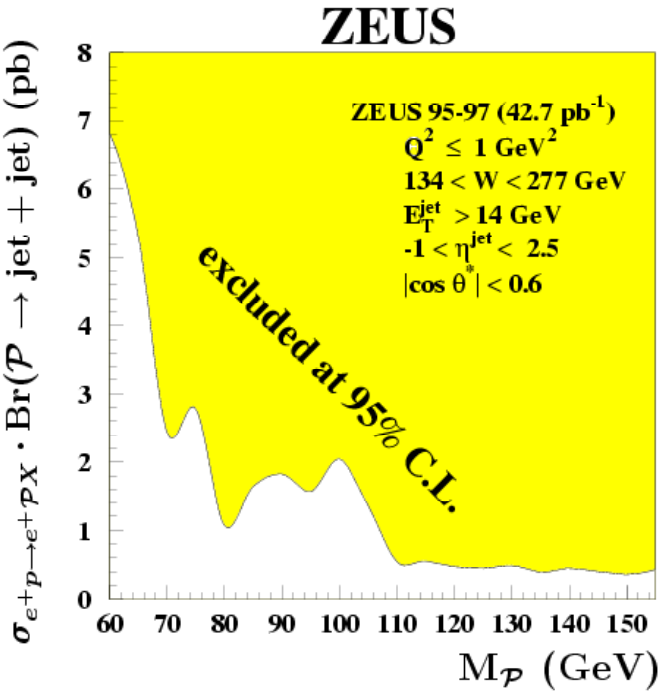

Figure 26: ZEUS excluded region of cross−section times branching ratio for new heavy resonances, P (see text).

6. Future plans and resources required

The first phase of HERA running, prior to the upgrade which has recently been completed, has established HERA as the place to study proton structure in the region of low-*x* and, increasingly, to test assumptions made at high-*x*. Commissioning of the upgraded accelerator and detector is now underway. We anticipate that over the course of running at HERA II we shall accumulate five times more data than we accumulated over the years 1992 — 2000 and that these data will allow us to extend the range of QCD and electroweak measurements which can be performed as well as enhancing the search capabilities beyond the Standard Model.

The ability to tag heavy flavours using the MVD and the ability to measure precisely the polarisation of the lepton beams using the TPOL will greatly improve these studies. The future programme builds upon existing ZEUS-UK analyses as well as the investment in the MVD and TPOL. Over the next two years we shall begin to reap the reward of these investments by developing the leading role we have established in the areas of high-Q^2 DIS cross section measurements, heavy flavour tagging, QCD studies of the hadronic final state and searches for physics beyond the Standard Model.

The resources requested are summarised in the following table.

	Estimates	**Forward Look**		
FUNDS (£K)	**2002/03**	**2003/2004**	**2004/05**	**2005/06**
Maint. & Running Costs	**181**	**200**	**200**	**200**

Travel − Long Term	**110**	**110**	**110**	**110**
Travel − Short Term	**120**	**120**	**120**	**120**
TOTAL	**411**	**430**	**430**	**430**
Exchange Rate Element: ZEUS common fund, billed in Euros.	**120**	**150**	**150**	**150**
RAL EFFORT (SY)				
Instrumentation Division (formerly Tech/Electronics)	**0.5**	**0.5**	**0.5**	**0.5**

Table 2: Resources requested for continued support of ZEUS UK.

References

[1] T. Matsushita *et al., Optical alignment system for the ZEUS microvertex detector,* Nucl. Instr. Meth. **A466** (2001) 383−389.

[2] Future Physics at HERA vol. 1, 127−236, Workshop on Future Physics at HERA, Hamburg, Germany, 25−26 Sep. 1995.

[3] F. Zetsche, *Lepton Beam Polarisation at HERA,* Future physics at HERA, vol. 1, 222−226, Hamburg 1996.

[4] Zhi−qing Zhang, Electron Polarisation Measurement using a Fabry−Perot Cavity at HERA (Orsay, LAL). LAL−01−87, PRHEP−HEP2001−261, Dec 2001. 5pp.

[5] R.J. Cashmore *et.al., Measurement of Weak Neutral Current Couplings of Quarks at HERA,* Future physics at HERA 163−189, Workshop on Future Physics at HERA, Hamburg, Germany, 30−31 May 1996.

[6] ZEUS Collaboration, S. Chekanov *et al., A ZEUS next−to−leading−order QCD analysis of data on deep inelastic scattering,* forthcoming.

[7] ZEUS Collaboration, S.Chekanov et al., *Measurement of the neutral current cross−section and F_2 structure function for deep inelastic e^+p scattering at HERA,* Eur. Phys. J. **C21** (2001) 443.

[8] A.D.Martin *et al.,* hep−ph/0110215.

[9] J. Pumplin *et al.,* hep−ph/0201195.

[10] ZEUS Collaboration, J.Breitweg *et al., Measurement of the Proton Structure Function F_2 at Very Low Q^2 at HERA* Phys. Lett. **B487** (2000) 53.

[11] ZEUS Collaboration, J.Breitweg et al., *Measurement of High Q^2 Charged−Current e^+ p Deep Inelastic Scattering Cross Sections at HERA,* Eur. Phys. J. **C12** (2000) 411.

[12] ZEUS Collaboration, S. Chekanov *et al., Measurement of High−Q^2 neutral current cross sections in e^-p deep inelastic scattering at HERA,*forthcoming.

[13] ZEUS Collaboration, S. Chekanov *et al., Measurement of High−Q^2 charged current cross sections in e^-p deep inelastic scattering at HERA,* accepted by Phys. Lett.

[14] ZEUS Collaboration, *Measurement of high−Q^2 neutral current cross sections in e^+p deep inelastic scattering at HERA,* Abstract 630 submitted to the International Europhysics Conference on High Energy Physics July 12 − 18, 2001, Budapest, Hungary.
ZEUS Collaboration, *Measurement of high−Q^2 charged current cross sections in e^+p deep inelastic scattering at HERA,* Abstract 631 submitted to the International Europhysics Conference on High Energy Physics July 12 − 18, 2001, Budapest, Hungary.

[15] ZEUS Collaboration, J. Breitweg *et al., Measurement of $D^{*\pm}$ production and the charm contribution to F_2 in deep inelastic scattering at HERA,* The European Physical Journal C12 (2000) 35.

[16] ZEUS Collaboration, J. Breitweg *et al., Measurement of inclusive $D^{*\pm}$ and associated dijets cross sections in photoproduction at HERA*, The European Physical Journal **C6** (1999) 67.

[17] ZEUS Collaboration, J. Breitweg *et al., Measurement of open beauty production in photoproduction at HERA*, The European Physical Journal **C18** (2001) 625.

[18] R. Waugh, Glasgow University PhD Thesis (1999);
G. McCance, "Event Shapes at HERA", Moriond (2000) Proceedings ;
G. McCance, Glasgow University Ph.D. Thesis (2000)

[19] E.A.Heaphy, *Three−jet Production at HERA*, Durham Workshop on Collider Physics, (Sept. 1999)

[20] ZEUS Collaboration, J. Breitweg et al., *Measurement of three− jet distributions in photoproduction at HERA*; Phys.Lett.**B443** (1998) 394−408.

[21] ZEUS Collaboration, S Chekanov et al.,*Dijet photoproduction at HERA and structure of the photon*, DESY−01−220 submitted to Eur. Phys. J.

[22] ZEUS Collaboration, J.Breitweg et al., *The Q^2 Dependence of Dijet Cross Sections in γp Interactions at HERA* Phys. Lett. **B479** (2000) 37;
N.MacDonald, Glasgow University PhD Thesis (1999).

[23] T.Sjöstrand and G.A.Schuler; Z. Phys. **C68** (1995) 607.

[24] S.Boogert; *Photoproduction of neutral strange hadrons at ZEUS*; Photon 2001 2−7 Sept 2001, Ascona, Switzerland.

[25] ZEUS Collaboration, J. Breitweg et al., *Observation of isolated high E_T photons in photoproduction at HERA*, Phys.Lett.**B413** (1997) 201.

[26] ZEUS Collaboration, J. Breitweg et al., *Measurement of inclusive prompt photon photoproduction at HERA* , Phys.Lett.**B472** (2000) 175.

[27] ZEUS Collaboration, S Chekanov et al., *High−mass dijet cross sections in photoproduction at HERA*, DESY 01−219, submitted to Phys. Lett.

[28] S.Weinberg; Phys. Rev. **D19** (1979) 1277;
L.Susskind; Phys. Rev. **D20** (1979) 2619;

A ZEUS Publications since May 2000

- ZEUS Collaboration; S. Chekanov et al.
  Measurement of diffractive production of D^{*+-} (2001) mesons in deep inelastic scattering at HERA
  DESY−02−082 (June 2002)
  submitted to Physics Letters B

- ZEUS Collaboration; S. Chekanov et al.
  Measurement of proton−dissociative diffractive photoproduction of vector mesons at large momentum transfer at HERA
  DESY−02−072 (May 2002)
  submitted to The European Physical Journal C

- ZEUS Collaboration; S. Chekanov et al.
  Measurement of high− Q^2 charged current cross sections in e^-p deep inelastic scattering at HERA
  DESY−02−064 (May 2002)
  accepted by Physics Letters B

- ZEUS Collaboration; S. Chekanov et al.
  Leading Neutron production in e^+p collisions at HERA
  DESY−02−039 (April 2002)
  accepted by Nucl. Physics B

- ZEUS Collaboration; S. Chekanov et al.
  Measurement of the Q^2 and energy dependence of diffractive interactions at HERA
  DESY−02−029 (March 2002)
  accepted by Europ. Phys. Journal C

- ZEUS Collaboration; S. Chekanov et al.
  Exclusive photoproduction of J/Psi mesons at HERA
  DESY−02−008 (January 2002)

- ZEUS Collaboration; S. Chekanov et al.
  Search for lepton−flavor violation in e^+p collisions at HERA
  DESY−01−222 (December 2001)
  accepted by Phys. Rev. D

- ZEUS Collaboration; S. Chekanov et al.
  Dijet photoproduction at HERA and the structure of the photon
  DESY−01−220 (December 2001)
  The European Physical Journal C23 (2002) 4, 615−631

- ZEUS Collaboration; S. Chekanov et al.
  High−mass dijet cross sections in photoproduction at HERA

DESY 01−219 (December 2001)
Physics Letters B531 (2002) 9−27

- ZEUS Collaboration; S. Chekanov et al.
Measurement of the photon−proton total cross section at a center−of−mass energy of 209 GeV at HERA
DESY−01−216 (December 2001)
Nuclear Physics B627 (2002) 3−28

- ZEUS Collaboration; S. Chekanov et al.
Searches for excited fermions in ep collisions at HERA
DESY−01−132 (September 2001)
submitted to Physics Letters B

- ZEUS Collaboration; S. Chekanov et al.
Dijet production in neutral current deep inelastic scattering at HERA
DESY−01−127 (August 2001)
The European Physical Journal C23 (2002) 1, pp 13−27

- ZEUS Collaboration; S. Chekanov et al.
Properties of hadronic final states in diffractive deep inelastic scattering at HERA
DESY−01−097 (July 2001)
Phy. Rev. D65, 052001 (2002)

- ZEUS Collaboration; S. Chekanov et al.
Three−jet production in diffractive deep inelastic scattering at HERA
DESY−01−092 (June 2001)
Physics Letters B 516 (2001) 3−4, pp 273−292

- ZEUS Collaboration; S. Chekanov et al.
Measurement of the neutral current cross section and F_2 structure function for deep inelastic e^+p scattering at HERA
DESY−01−064 (May 2001)
The European Physical Journal C 21 (2001) 3, pp 443−471

- ZEUS Collaboration; S. Chekanov et al.
Multiplicity moments in deep inelastic scattering at HERA
DESY 01−053 (April 2001)
Physics Letters B 510 (2001) 36−54

- ZEUS Collaboration; S. Chekanov et al.
Study of the effective transverse momentum of partons in the proton using prompt photons in photoproduction at HERA
DESY 01−043 (March 2001)
Physics Letters B 511 (2001) 19−32

- ZEUS Collaboration; J. Breitweg et al.
Measurement of dijet production in neutral current deep inelastic scattering at high Q^2 and

determination of α_s
DESY 01−018 (February 2001)
Physics Letters B 507 (2001) 70−88

- ZEUS Collaboration; J. Breitweg et al.
Measurement of open beauty production in photoproduction at HERA
DESY 00−166 (November 2000)
The European Physical Journal C 18 (2001) 625−637

- ZEUS Collaboration; J. Breitweg et al.
Measurement of dijet cross sections for events with a leading neutron in photoproduction at HERA
DESY 00−142 (October 2000)
Nuclear Physics B 596 (2001) 3−29

- ZEUS Collaboration; J. Breitweg ~~et~~ al.
A search for resonance decays to ν*−jet in* e^+p *scattering at HERA*
DESY 00−133 (September 2000)
Physical Review D 63 (2001) Issue 5, Article # 052002

- ZEUS Collaboration; J. Breitweg et al.
Measurement of exclusive Ω *electroproduction at HERA*
DESY 00−084 (June 2000)
Physics Letters B 487 (2000) 3−4, 273−288

- ZEUS Collaboration; J. Breitweg et al.
Measurement of the Proton Structure Function F_2 *at Very Low* Q^2 *at HERA*
DESY 00−071 (May 2000)
Physics Letters B 487 (2000) 1−2, 53−73

B Conference talks by ZEUS UK members

Speaker	Conference	Venue	Date
D. Bailey	New Trends in HEP	Yalta, Ukraine	September 2001
D. Bailey	Int. Workshop on Ageing Phenomena in Gaseous Detectors	DESY, Germany	October 2001
N. Brook	HEP IoP	Edinburgh, UK	April 2000
N. Brook	DIS 2000	Liverpool, UK	April 2000
N. Brook	ICHEP 2000	Osaka, Japan	July 2000
N. Brook	New Trends in HERA Physics	Tegernsee, Germany	June 2001
N. Brook (workshop organiser)	UK Phenomenology Workshop	Durham, UK	December 2001
J. Cole	QFTHEP'2001	Moscow, Russia	September 2001
B. Foster	Korean Physical Soc.	Seoul, Korea	March 2001
B. Foster	DIS 2001	Bologna, Italy	April 2001
B. Foster	Hellenic Summer School	Corfu, Greece	August 2001
B. Foster	LHC01	Sardinia, Italy	October 2001
B. Foster	INFN Spring School 'Bruno Toushek'	Frascati, Italy	June 2002
B. Foster	Quark Nuclear Physics	Juelich, Germany	June 2002
S. Robins	DIS 2002	Krackow, Poland	May 2002
E. Rodrigues	Rencontres de Moriond.	Les Arcs, France	March 2002
J. Scott	DIS 2000	Liverpool, UK	April 2000
R.Tapper	Vietnam 2000	Hanoi, Vietnam	July 2000
M. Wing	New Trends in HERA Physics	Tegernsee, Germany	June 2001
M. Wing (convenor: Jet and Inclusive Hadron Production)	Photon'01	Ascona, Switzerland	September 2001
M. Wing	Calorimetry in High Energy Physics	Annecy, France	October 2000**M. Wing**Calorimetry in High Energy PhysicsPasadena, USAMarch 2002**M. Wing**IoP CongressBrighton, UKApril 2002

Speaker	Conference	Venue	Date
P. J. Bussey	UK Phenomenology workshop on heavy flavours and CP violation,	Durham, UK	2000
P. J. Bussey	UK Phenomenology workshop on heavy flavours and CP violation,	Durham, UK	2000
P. J. Bussey	DIS 2001	Bologna	2001
P. J. Bussey	Workshop on Skewed Parton Distribution and Lepton−Nucleon Scattering	DESY, Germany	2000
A. Doyle	7th Conference on Intersections between Particle and Nuclear Physics	Quebec, Canada	2000
C. Foudas	DIS 2002	Krakow, Poland	2002
K. Long	53rd DESY PRC 16 May, 2002, Open Session	Hamburg, Germany	2002
K. Long	INSTR02	Novosibirsk, Russia	February 2002
K. Long **Convener of structure function sessions**	DIS 2001	Bologna, Italy	April 2001
K. Long	8th International Workshop on Deep Inelastic Scattering and QCD (DIS2000)	Liverpool, UK	April 2000
K. Long	*ep* interactions at high E_T	KEK, Tskuba, Japan	March 2000
A. Tapper	Fundamental Interactions Lake Louise Winter Institute	Alberta, Canada	2001
F. Metlica	Particle Physics 2001	Southampton, UK	2001
F. Metlica	DIS 2002	Krakow, Poland	2002
R . Walczak	Nordic meeting on particle physics	Oslo, Norway	2000
E. A. Heaphy	8th International Workshop on Deep Inelastic Scattering and QCD (DIS2000)	Liverpool, UK	2000
E. A. Heaphy	XXXI International Symposium on Multiparticle Dynamics	Datong, Shanxi Province, China.	2001

O. Ruske	Moriond Conference on QCD and High Energy Hadronic Interactions	Moriond, France	2000

Speaker	**Conference**	**Venue**	**Date**
R. C. E. Devenish	DESY Theorie Workshop on CP Violation and B Physics	DESY−Hamburg, Germany	2000
R. C. E. Devenish	Physics in Collision	Stanford University, USA	June 2002
A M Cooper−Sarkar	Invited talk at ISMD2000	Lake Balaton, Hungary	2000
A M Cooper−Sarkar	Invited talk at EuroHEP01	Budapest, Hungary	2001
A M Cooper−Sarkar	IPPP Workshop on Advanced Statistical Methods in HEP	Durham, UK	2002
A M Cooper−Sarkar	Convenor and summary speaker on Structure Functions at DIS2002	Krakow, Poland	2002
M R Sutton	15th High−Energy Physics Int'l Euroconference on QCD	Montpellier, France	2000
M R Sutton	XVIth Int. Workshop in HEP & Quantum Field Theory	Moscow, Russia	2001
S Boogert	Photon2001	Ascona, Switzerland	2001
C.M Cormack	ICHEP 2000	Osaka, Japan	2000
C.M Cormack	CIPANP 2000	Quebec, Canada	2000
C.M Cormack	EPS 2001	Budapest, Hungary	2001
C.M Cormack	PIC 2001	Seoul, Korea	2001
J.C. Hart	Moriond QCD Conference	Les Arcs, France	2001
B. J. West	PHOTON 2001	,Ascona, Switzerland.	2001
J. M. Butterworth	51st DESY PRC 17 May, 2001, Open Session	Hamburg, Germany	2001

J. M. Butterworth	ICHEP 2000, XXXth International Conference on High Energy Physics	Osaka, Japan	2000

C.1 UK PhD Theses

(Submitted after May 2000)

Name	Institution	Date	Thesis Topic
J. Scott	**Bristol**	2000	*First Direct Measurement of F_L using ISR Events in Deep Inelastic Scattering at HERA.*
E. Rodrigues	**Bristol**	2001	*Azimuthal Angle Asymmetries of Hadrons and Jets in Deep Inelastic Scattering at HERA.*
S. Lee	**Glasgow**	2000	*Measurements of prompt photon production at HERA.*
G. McCance	**Glasgow**	2001	*Event Shapes and Power Corrections at HERA.*
A. Tapper	**Imperial**	2001	*Measurement of charged current deep inelastic scattering cross sections using the ZEUS detector at HERA*
O. Ruske	**Oxford**	2000	*Measurement and Phenomenology of the Proton Structure Function F_2 using the 1996 and 1997 ZEUS data at HERA*
B. West	**UCL**	2001	*Charm and the Virtual Photon at HERA and a Global Tracking Trigger for ZEUS*
E. Heaphy	**UCL**	2001	*Dijet Photoproduction and Photon Structure*